



TOTAL IONIZING DOSE TEST REPORT

No. 04T-RTSX72S(U)-D0YMJ1

September 1, 2004

J.J. Wang

(650) 318-4576

jih-jong.wang@actel.com

I. SUMMARY TABLE

Parameter	Tolerance
1. Gross Functionality	Passed 100 krad (Si)
2. Power Supply Current (I_{CCA}/I_{CCI})	Passed 57.6 krad (Si) per 25-mA spec. Post 100 krad (Si) and after 15 days room temperature annealing: average I_{CCA} = 172.6 mA; average I_{CCI} = 96.2 mA.
3. Input Threshold (V_{TIL}/V_{IH})	Passed 100 krad (Si)
4. Output Drive (V_{OL}/V_{OH})	Passed 100 krad (Si)
5. Propagation Delay	Passed 100 krad (Si) for 10% degradation criterion
6. Transition Time	Passed 100 krad (Si)

II. TOTAL IONIZING DOSE (TID) TESTING

This testing is designed on the base of an extensive database (see, for example, TID data of antifuse-based FPGA in <http://www.klabs.org/>) accumulated from the TID testing of many generations of antifuse-based FPGAs. One distinctive quality about this testing is the bench measurement of electrical parameters. Compared to an automatic-tester measurement, the bench measurement provides lower noise, better accuracy and more flexibility. The bench measurement samples pins for some measurements (e.g. threshold voltage measurement). However, since the tolerance is determined by the most degraded parameter, which is I_{CC} or propagation delay, sampling the pins for measuring non-critical parameters is appropriate.

A. Device Under Test (DUT) and Irradiation Parameters

Table 1 lists the DUT and irradiation parameters. During irradiation each input or output is grounded through a 1-M ohm resistor; during annealing each input or output is grounded through a 1-k ohm resistor. Appendix A contains the schematics of the bias circuit.

Table 1 DUT and Irradiation Parameters

Part Number	RTSX72SU
Package	CQFP256
Foundry	United Microelectronics Corp.
Technology	0.25 μ m CMOS
DUT Design	TDSX72CQFP256_2Strings
Die Lot Number	D0YMJ1
Quantity Tested	4
Serial Number	39765, 39770, 39792, 39843, 39845
Radiation Facility	Defense Microelectronics Activity
Radiation Source	Co-60
Dose Rate	1 krad (Si)/min ($\pm 5\%$)
Irradiation Temperature	Room
Irradiation and Measurement Bias (V_{CCI}/V_{CCA})	Static at 5.0 V/2.5 V

B. Test Method

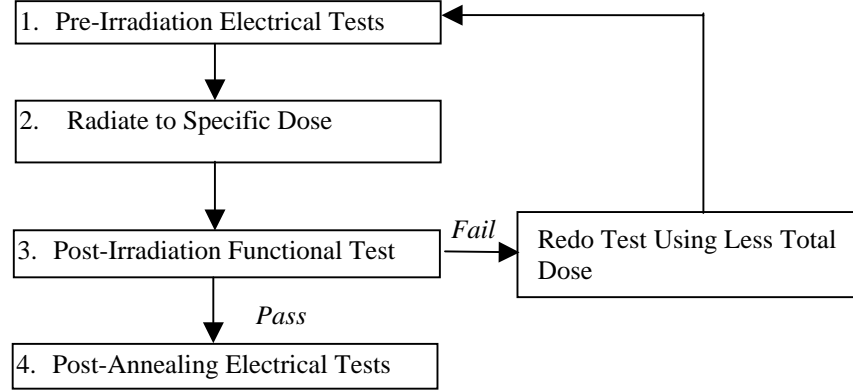


Figure 1 Parametric test flow chart

The test method generally follows the guidelines in the military standard TM1019. Figure 1 is the flow chart showing the steps for parametric tests, irradiation, and post-irradiation annealing.

The accelerated aging, or rebound test mentioned in TM1019 is unnecessary because there is no adverse time dependent effect (TDE) in products manufactured by sub-micron CMOS technology. To prove this point, test data using a high dose rate (1 krad (Si)/min) are compared with test data using a low dose rate (1 krad (Si)/hr) for devices manufactured by several generations of sub-micron CMOS technologies. Since the results always show the low-dose-rate degradation less than the high-dose-rate degradation, the elevated rebound annealing would artificially improve the electrical parameters. Therefore, only room temperature annealing is performed in this report. DUTs are biased annealed for 15 days after the 100-krad (Si) irradiations.

C. Design and Parametric Measurements

DUTs use a high utilization generic design (TDSX72CQ256_2Strings) to test total dose effects in typical space applications. Appendix B contains the schematics illustrating the logic design.

Table 2 lists each electrical parameter and the corresponding logic design. The functionality is measured on the output pins (O_AND3 and O_AND4) of two combinational buffer-strings with 1400 buffers each and output pins (O_OR4 and O_NAND4) of a shift register with 1536 bits. I_{CC} is measured on the power supply of the logic-array (I_{CCA}) and I/O (I_{CCI}) respectively. The input logic thresholds (V_{TIL}/V_{IH}) and output-drive voltages (V_{OL}/V_{OH}) are measured on a combinational net, the input pin DA to the output pin QA0. The propagation delays are measured on the O_AND4 output of one buffer string. The delay is defined as the time delay from the time of triggering edge at the CLOCK input to the time of switching state at the output O_AND4. Both the low-to-high and high-to-low output transitions are measured; the propagation delay is defined as the average of these two transitions. The transition characteristics, measured on the output O_AND4, are displayed as oscilloscope snapshots showing the rising and falling edge during logic transitions.

Table 2 Logic Design for Parametric Measurements

Parameters	Logic Design
1. Functionality	All key architectural functions (pins O_AND3, O_AND4, O_OR3, O_OR4, and O_NAND4)
2. I_{CC} (I_{CCA}/I_{CCI})	DUT power supply
3. Input Threshold (V_{TIL}/V_{IH})	Input buffer (pin DA to QA0)
4. Output Drive (V_{OL}/V_{OH})	Output buffer (pin DA to QA0)
5. Propagation Delay	String of buffers (pin LOADIN to O_AND4)
6. Transition Characteristic	D flip-flop output (O_AND4)

III. TEST RESULTS

A. Functionality

Every DUT passes the pre-irradiation, post-irradiation, and post-annealing functional tests.

B. Power Supply Current (I_{CCA} and I_{CCI})

Since the pre-irradiation I_{CCA} and I_{CCI} of every DUT are below 1 mA, the in-flux I_{CC} -plots of Figure 2 to Figure 6 basically show the radiation-induced leakage current. The room temperature annealing effect on I_{CC} is shown by Table 3, where the post-annealing data compares with the post-irradiation data.

Table 3. Post Irradiation and Post-Annealing I_{CC}

DUT	I_{CCA} (mA)		I_{CCI} (mA)	
	Post-rad	Post-ann	Post-rad	Post-ann
39765	335.1	159	264.1	103
39770	324	164	249.4	99
39792	416	181	268.8	96
39843	299.6	187	199.7	85
39845	409.8	172	264.1	98

An empirical equation is used to extract the total dose tolerance. The critical total dose ($\gamma_{critical}$) for a 10-year mission to induce I_{CC} to 25 mA is obtained from the equation:

$$I_{CCA}(\gamma_{critical}) \times 0.32 + I_{CCI}(\gamma_{critical}) \times 0.29 = 25mA$$

Where $I_{CCA}(\gamma)$ and $I_{CCI}(\gamma)$ are in-flux currents when total dose equals to γ . Using the-worst-case in-flux currents degradation, which is DUT 39792 (Figure 4), the tolerance ($\gamma_{critical}$) is obtained as approximately 57.6 krad (Si). This equation produces a conservative tolerance because the process of a high-dose-rate irradiation plus annealing produces an I_{CC} higher than the I_{CC} produced by a consistent low-dose-rate irradiation process.

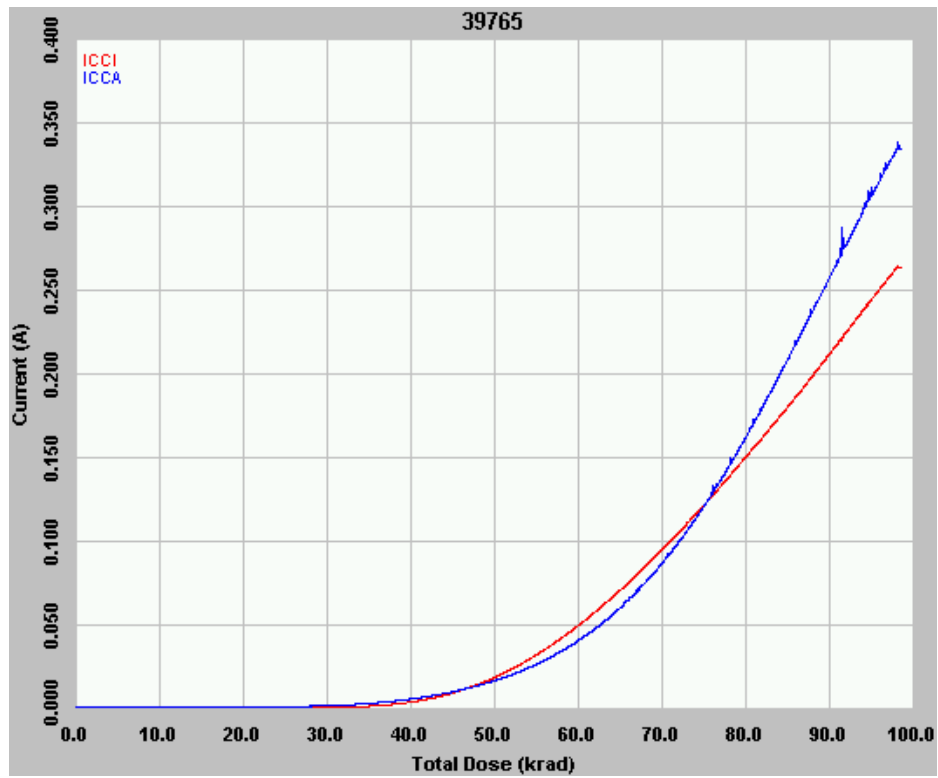


Figure 2 DUT 39765 in-flux I_{CCA} and I_{CCI}

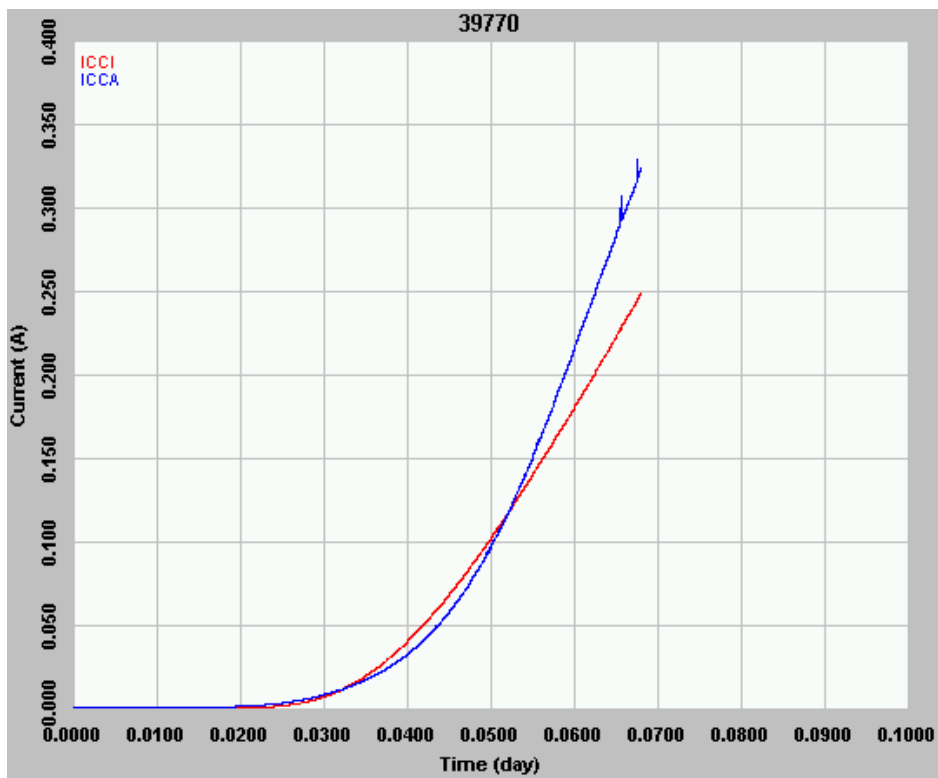


Figure 3 DUT 39770 in-flux I_{CCA} and I_{CCI}

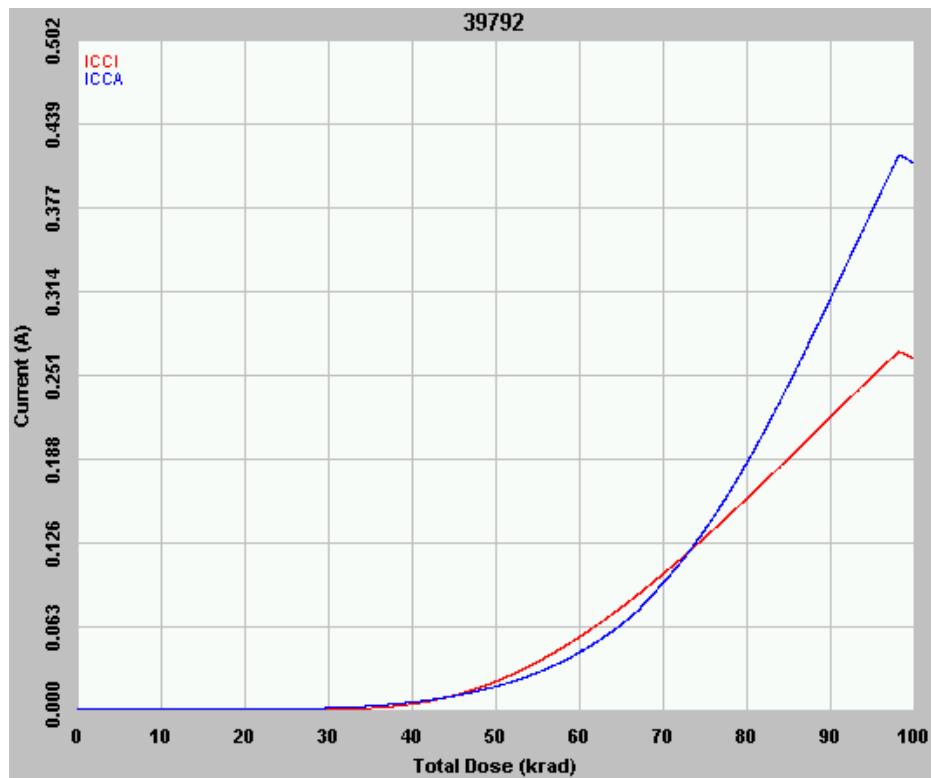


Figure 4 DUT 39792 in-flux I_{CCA} and I_{CCI}

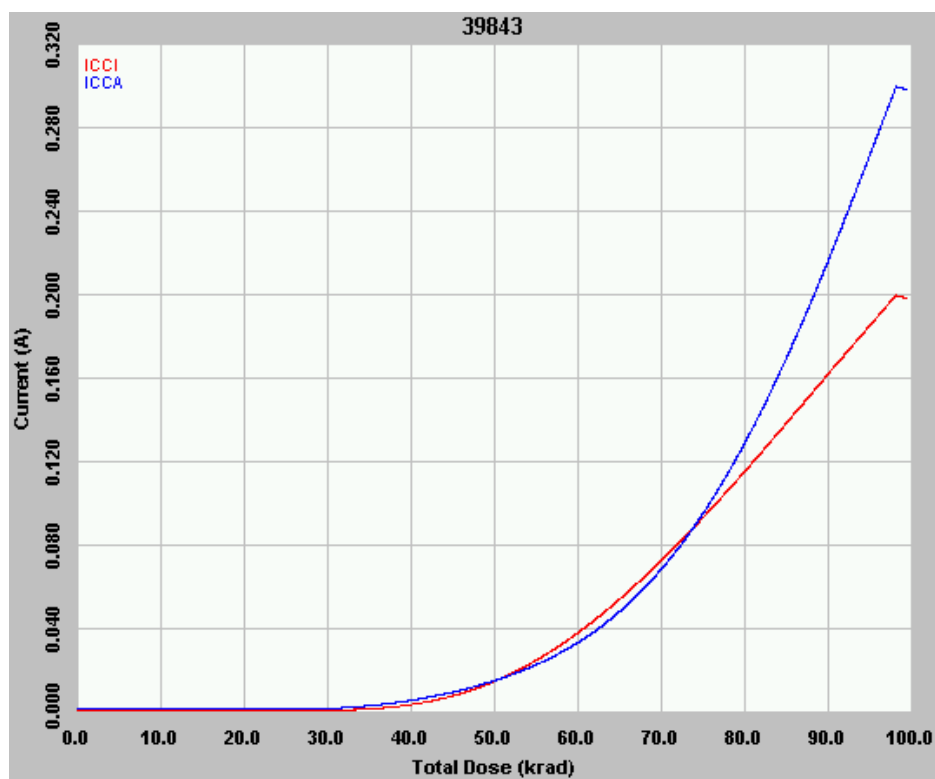


Figure 5 DUT 39843 in-flux I_{CCA} and I_{CCI}

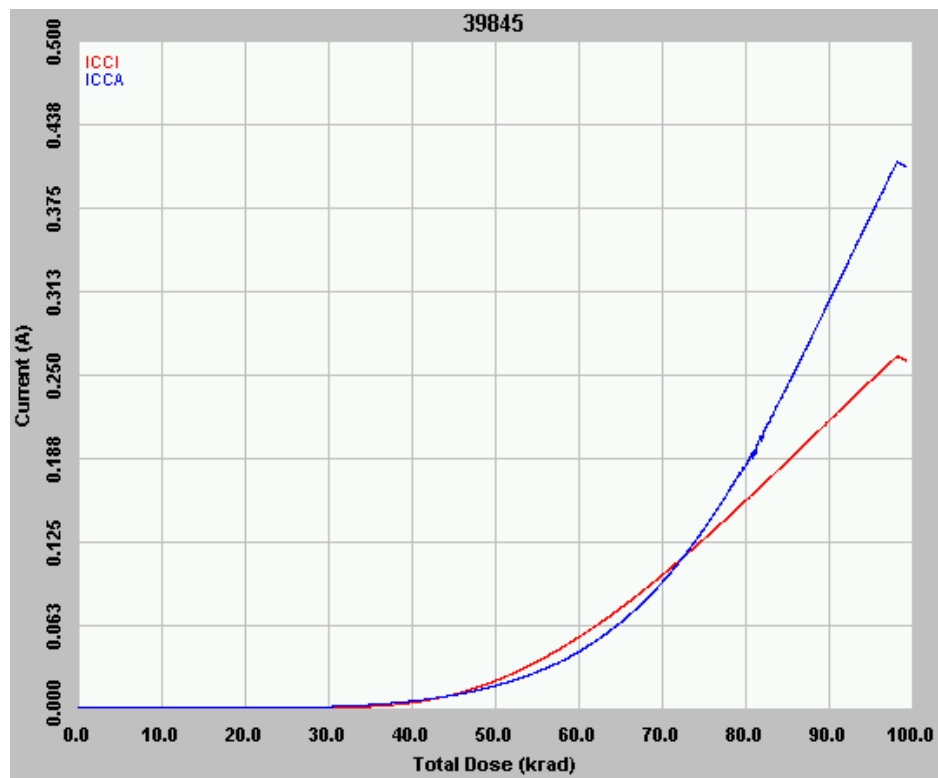


Figure 6 DUT 39845 in-flux I_{CCA} and I_{CCI}

C. Input Logic Threshold (V_{IL}/V_{IH})

Table 4 lists the pre-irradiation and post-annealing input logic threshold. All data are within the spec limits.

Table 4 Pre-Irradiation and Post-Annealing Input Thresholds

DUT	Pre-Irradiation		Post-Annealing	
	V_{IL} (V)	V_{IH} (V)	V_{IL} (V)	V_{IH} (V)
39765	1.33	1.49	1.31	1.54
39770	1.33	1.52	1.31	1.53
39792	1.32	1.49	1.22	1.49
39843	1.33	1.51	1.32	1.54
39845	1.33	1.51	1.23	1.49

D. Output-Drive Voltage (V_{OL}/V_{OH})

The pre-irradiation and post-annealing V_{OL}/V_{OH} are listed in Tables 5 and 6. The post-annealing data are within the spec limits; in each case, the post-annealing data varies minutely with respect to the pre-irradiation data.

Table 5 Pre-Irradiation and Post-Annealing V_{OL} (V) at Various Sinking Current

DUT	1 mA		12 mA		20 mA		50 mA		100 mA	
	Pre-rad	Pos-an	Pre-rad	Pos-an	Pre-rad	Pos-an	Pre-rad	Pos-an	Pre-rad	Pos-an
39765	0.009	0.010	0.103	0.108	0.172	0.179	0.433	0.450	0.890	0.925
39770	0.009	0.009	0.101	0.105	0.168	0.175	0.425	0.440	0.873	0.906
39792	0.009	0.010	0.102	0.110	0.169	0.184	0.427	0.463	0.879	0.954
39843	0.008	0.013	0.100	0.111	0.167	0.182	0.422	0.454	0.869	0.927
39845	0.009	0.010	0.102	0.108	0.170	0.179	0.431	0.451	0.885	0.927

Table 6 Pre-Irradiation and Post-Annealing V_{OH} (V) at Various Sourcing Current

DUT	1 mA		8 mA		20 mA		50 mA		100 mA	
	Pre-rad	Pos-an	Pre-rad	Pos-an	Pre-rad	Pos-an	Pre-rad	Pos-an	Pre-rad	Pos-an
39765	4.99	4.99	4.87	4.87	4.66	4.67	4.10	4.12	2.92	2.96
39770	4.99	4.98	4.87	4.87	4.66	4.67	4.12	4.14	2.96	3.00
39792	4.99	4.98	4.86	4.86	4.66	4.66	4.09	4.09	2.89	2.87
39843	4.99	4.99	4.87	4.88	4.66	4.68	4.12	4.14	2.95	3.00
39845	4.98	4.99	4.86	4.87	4.66	4.66	4.10	4.12	2.89	2.92

E. Propagation Delay

Table 7 lists the pre-irradiation and post-annealing propagation delays, and also lists the radiation-induced degradations in percentage. DUT 39845 has the worst degradation of 7.65%.

Table 7 Radiation-Induced Propagation Delay Degradations

DUT	Pre-Irradiation	Post-Annealing	Degradation
39765	1346.4	1421	5.54%
39770	1322.3	1397.9	5.71%
39792	1344.2	1434.9	6.74%
39843	1342.1	1433.4	6.80%
39845	1363.2	1467.6	7.65%

F. Transition Time

Figures 7 to 16 show the pre-irradiation and post-annealing transition edges. In each case, the radiation-induced transition-time degradation is not significant.

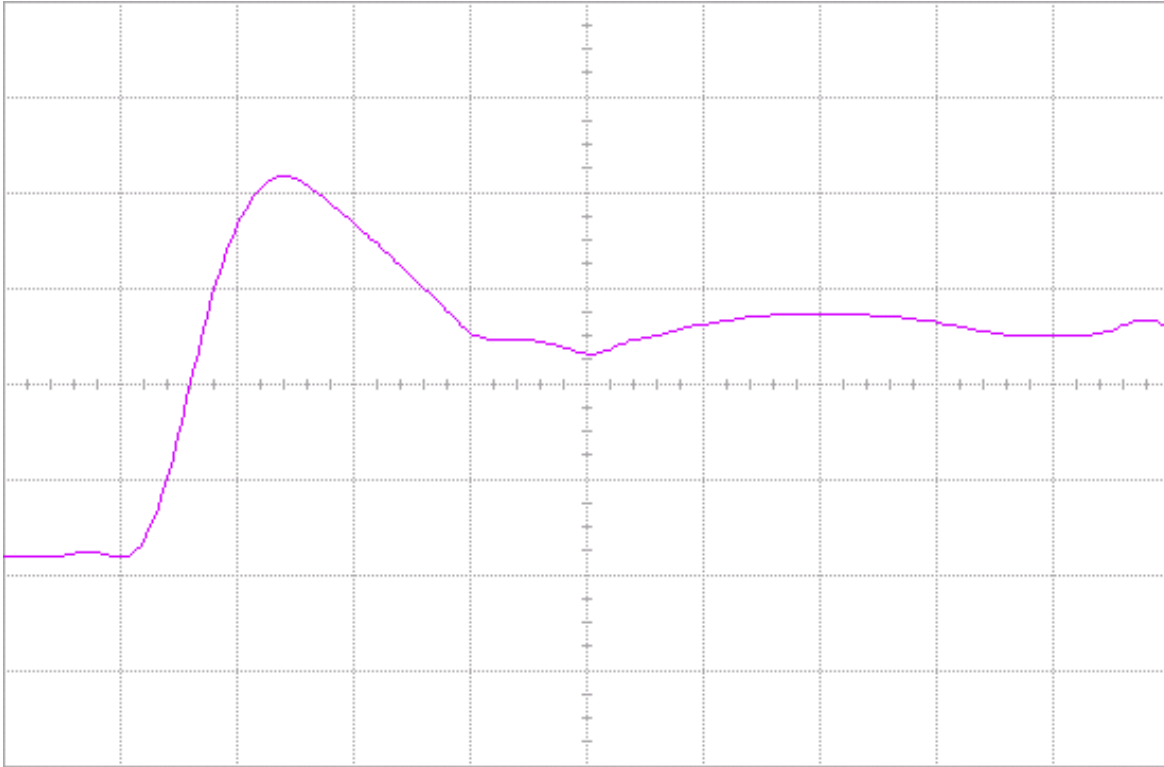


Figure 7(a) DUT 39765 pre-irradiation rising edge, abscissa scale is 2 V/div and ordinate scale is 2 ns/div.

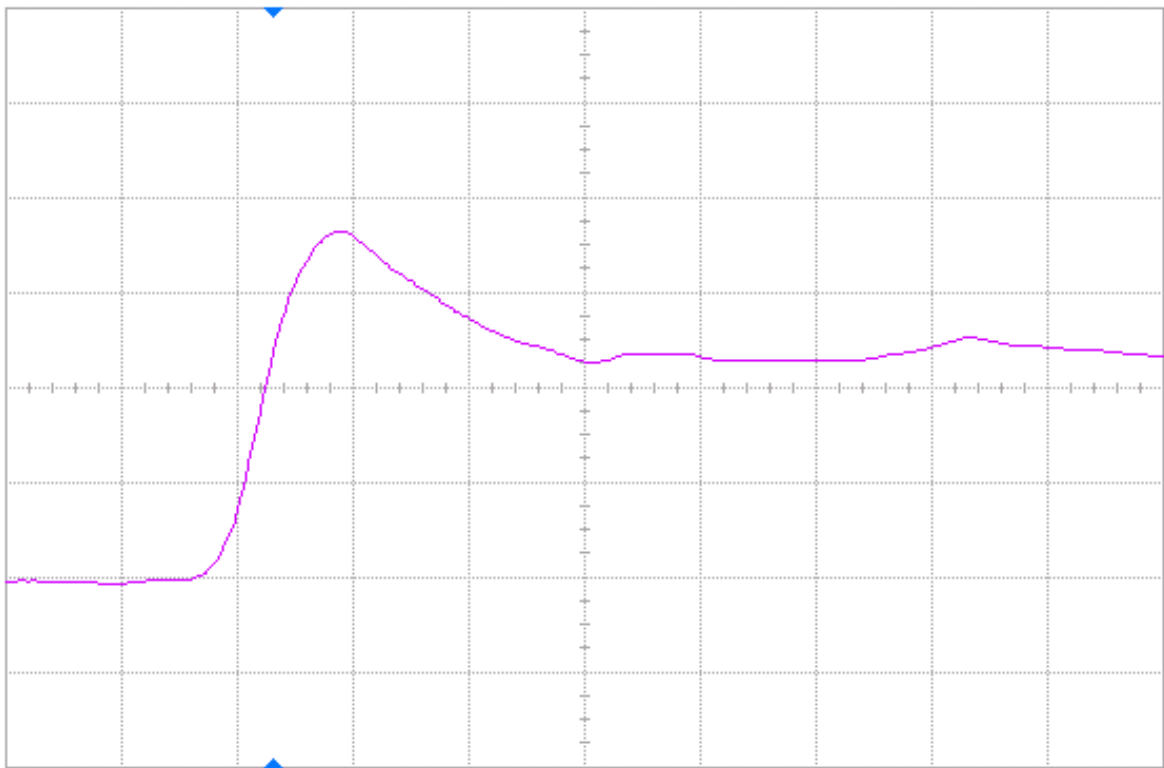


Figure 7(b) DUT 39765 post-annealing rising edge, abscissa scale is 2 V/div and ordinate scale is 2 ns/div.

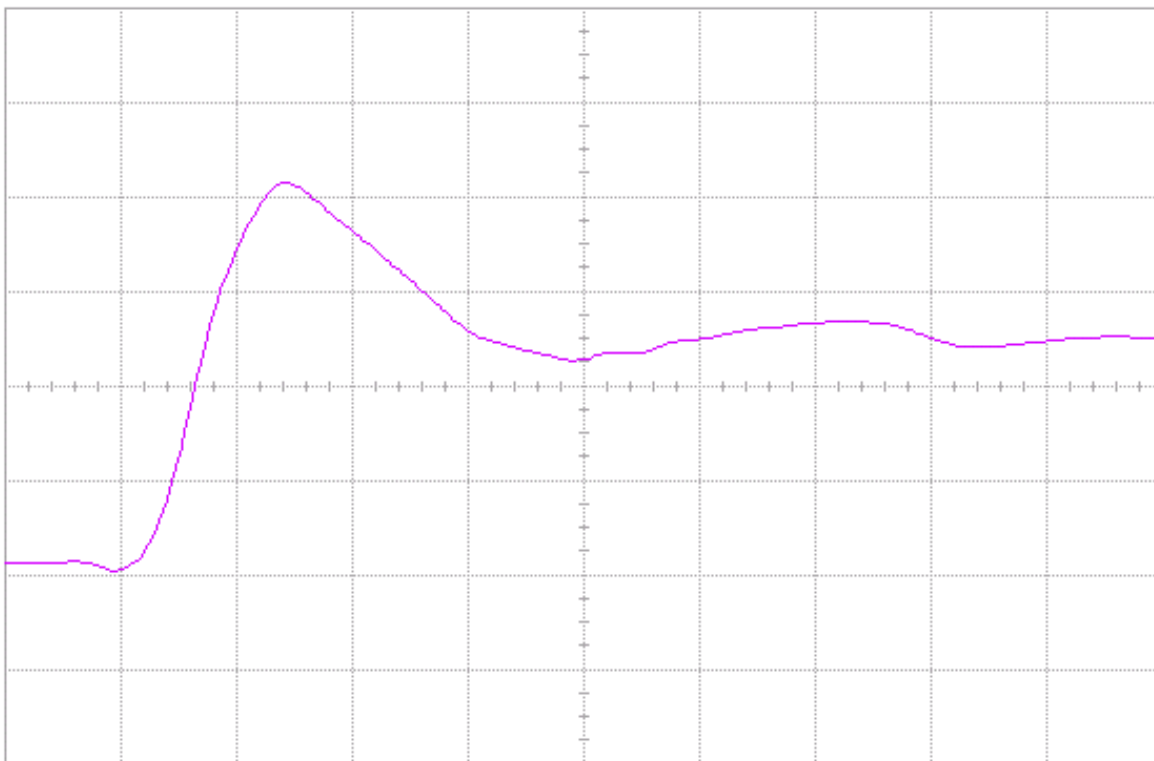


Figure 8(a) DUT 39770 pre-irradiation rising edge, abscissa scale is 2 V/div and ordinate scale is 2 ns/div.

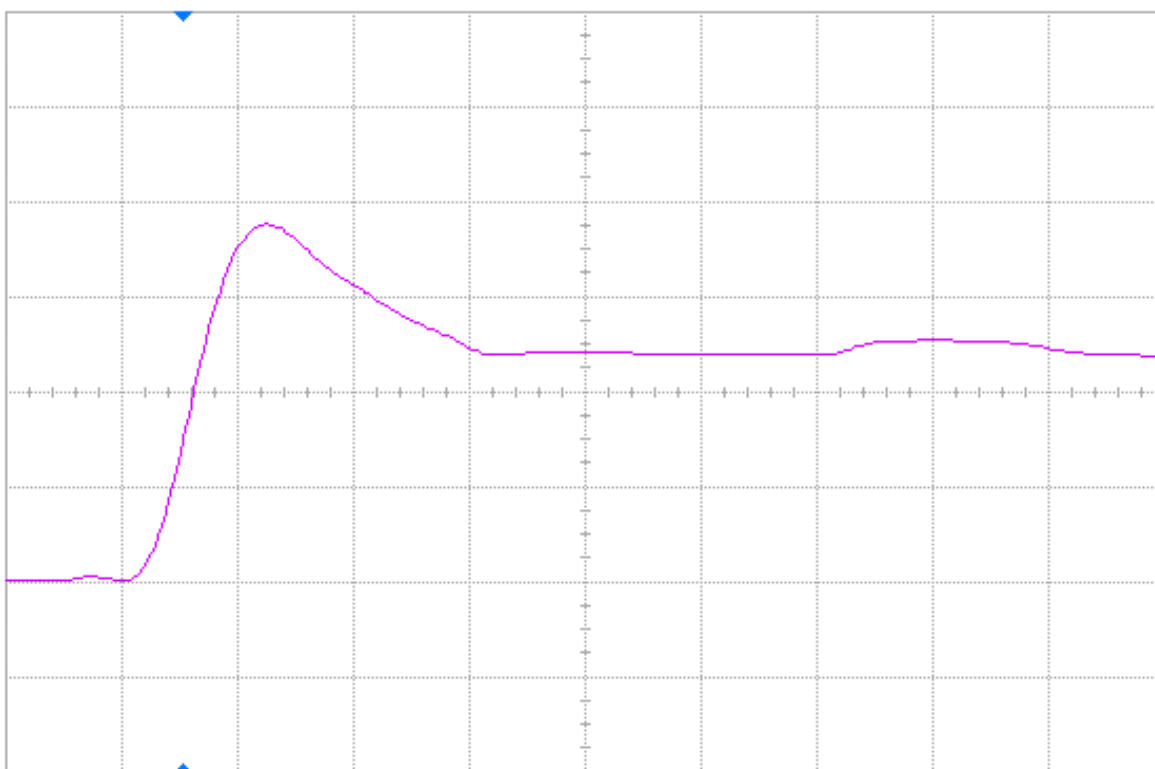


Figure 8(b) DUT 39770 post-annealing rising edge, abscissa scale is 2 V/div and ordinate scale is 2 ns/div.

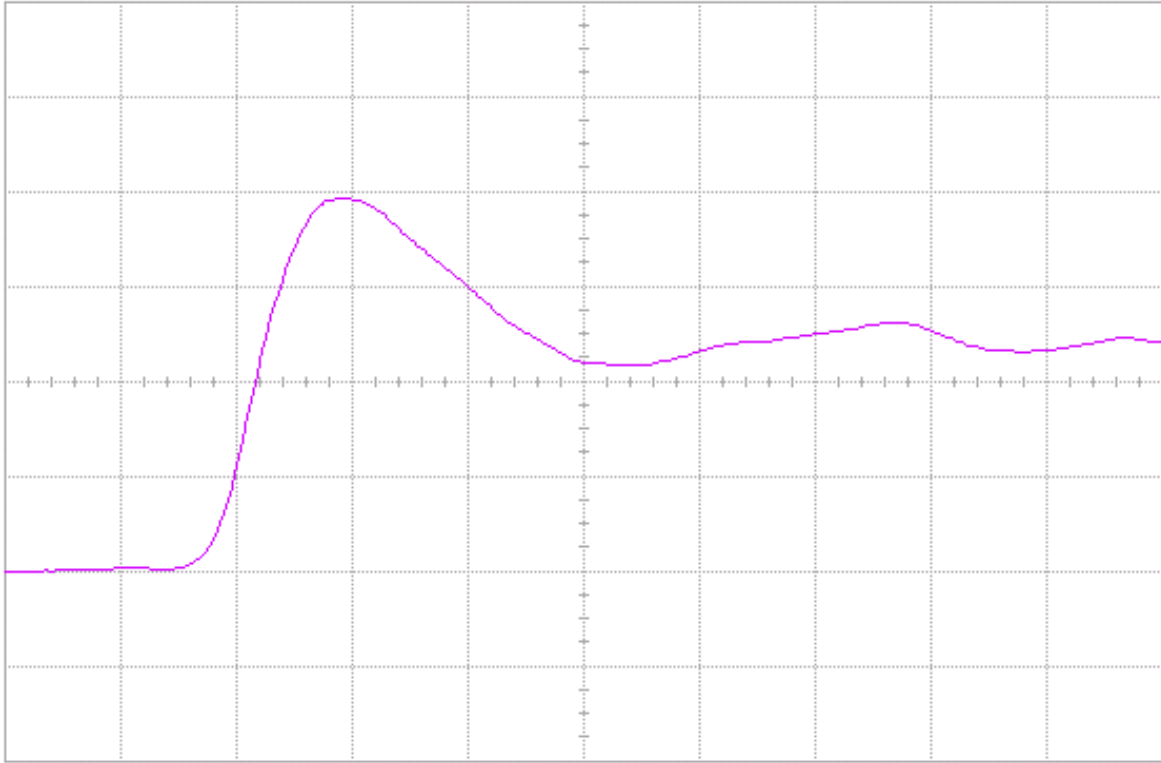


Figure 9(a) DUT 39792 pre-irradiation rising edge, abscissa scale is 2 V/div and ordinate scale is 2 ns/div.

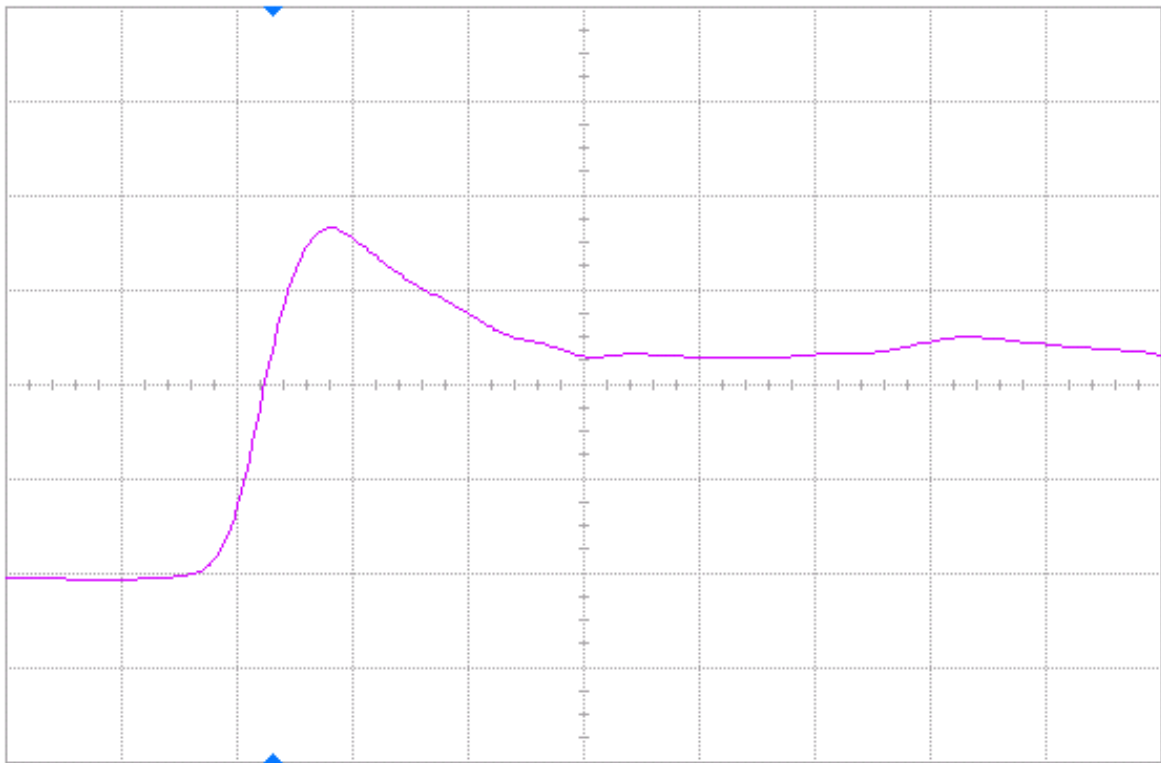


Figure 9(b) DUT 39792 post-annealing rising edge, abscissa scale is 2 V/div and ordinate scale is 2 ns/div.

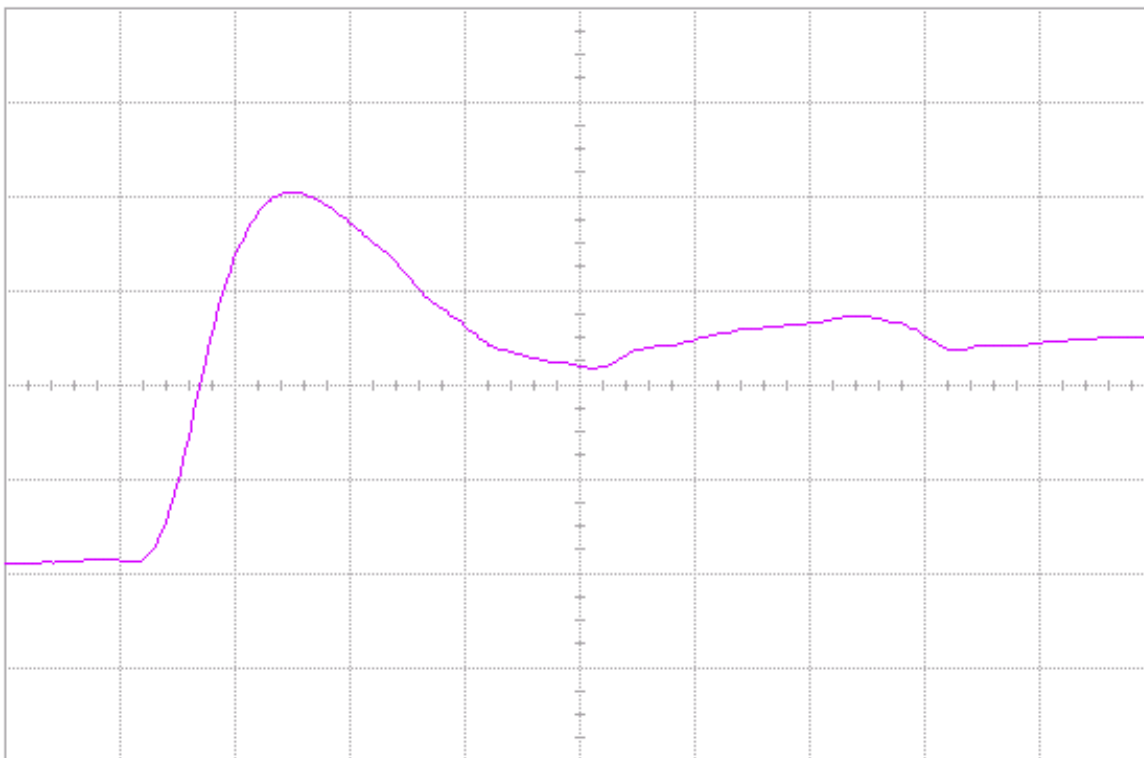


Figure 10(a) DUT 39843 pre-irradiation rising edge, abscissa scale is 2 V/div and ordinate scale is 2 ns/div.

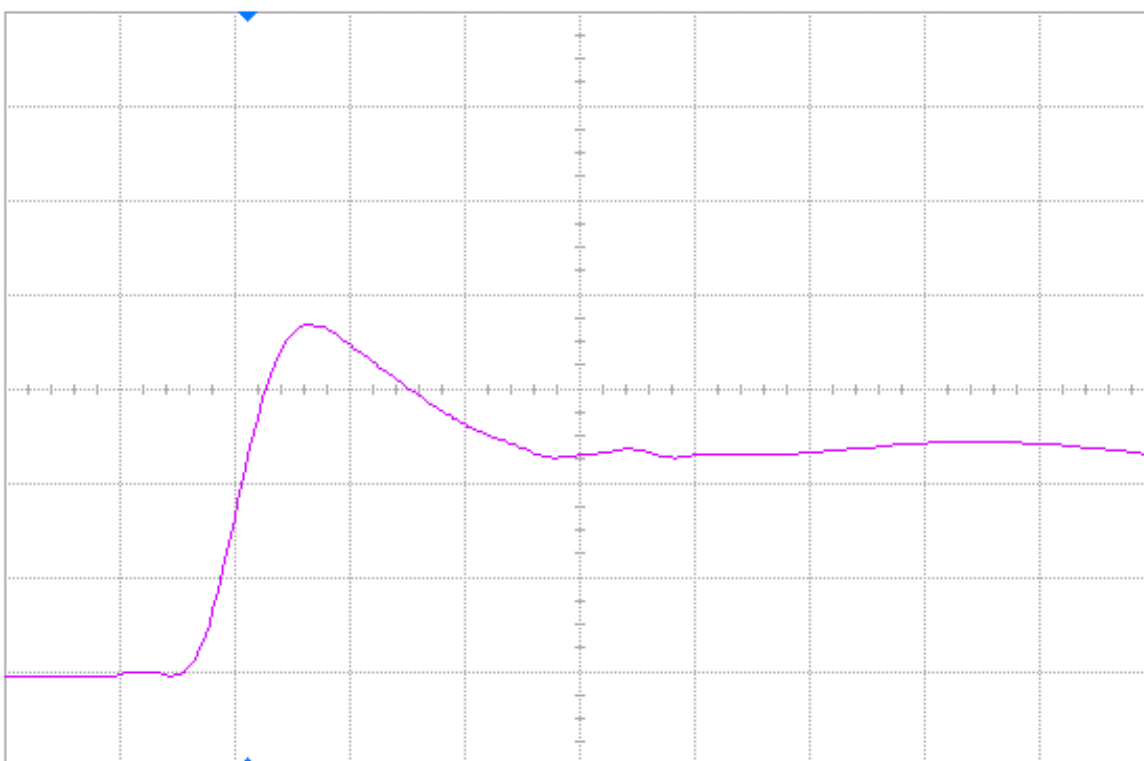


Figure 10(b) DUT 39843 post-annealing rising edge, abscissa scale is 2 V/div and ordinate scale is 2 ns/div.

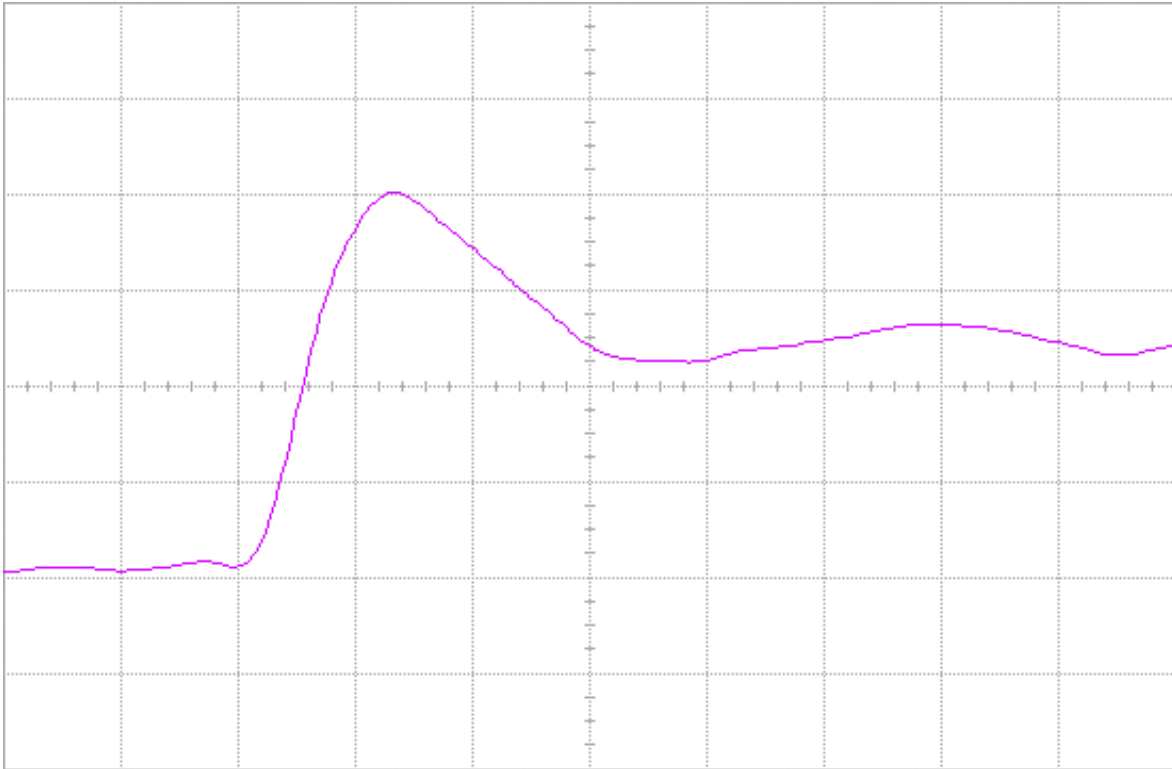


Figure 11(a) DUT 39845 pre-irradiation rising edge, abscissa scale is 2 V/div and ordinate scale is 2 ns/div.

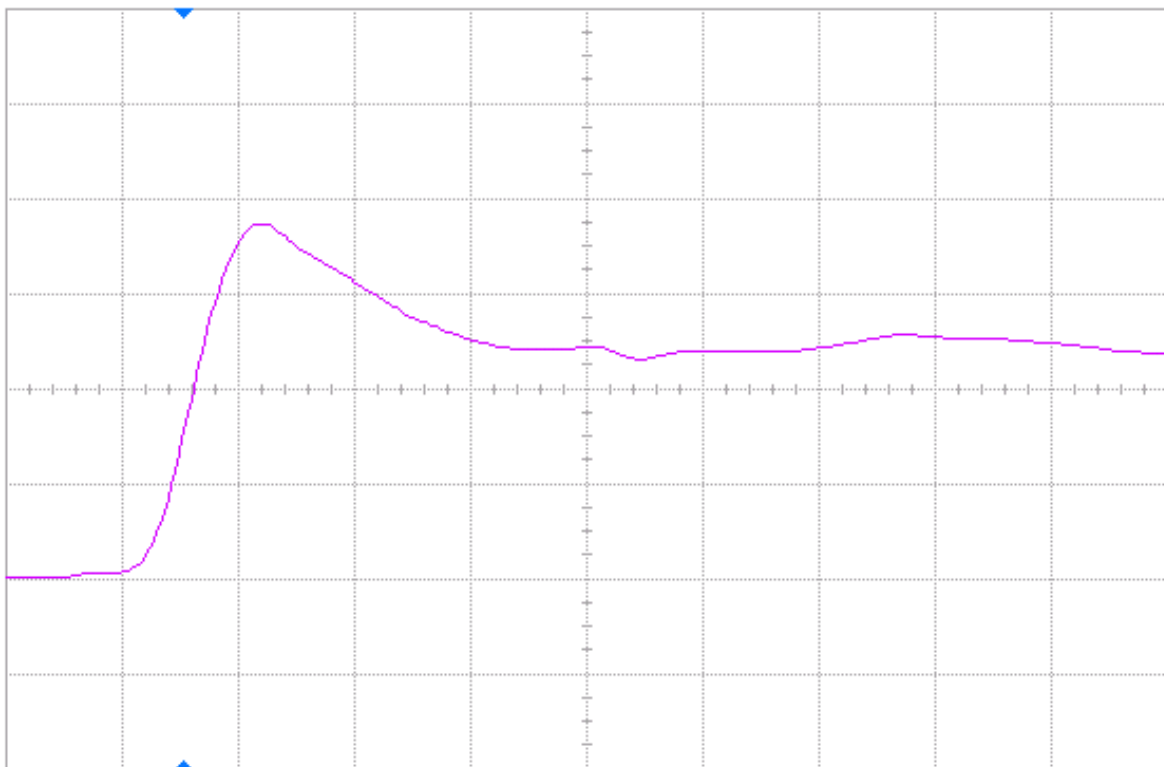


Figure 11(b) DUT 39845 post-irradiation rising edge, abscissa scale is 2 V/div and ordinate scale is 2 ns/div.

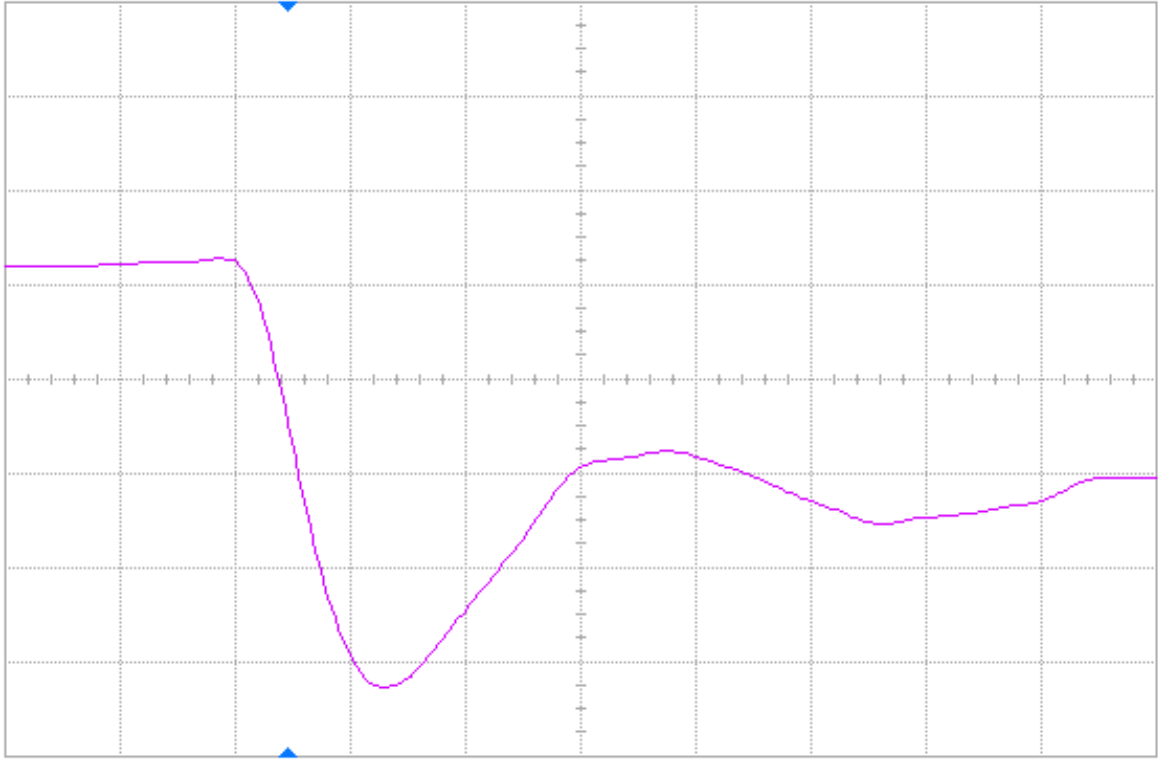


Figure 12(a) DUT 39765 pre-irradiation falling edge, abscissa scale is 2 V/div and ordinate scale is 2 ns/div.

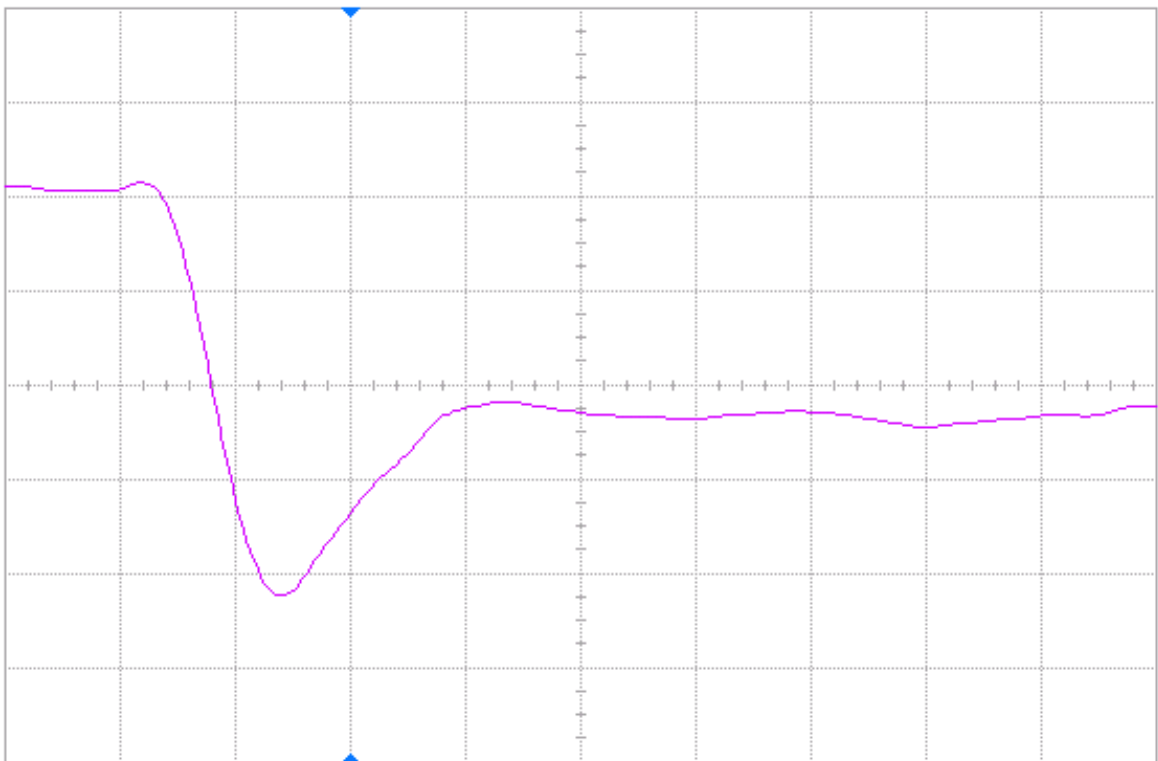


Figure 12(b) DUT 39765 post-annealing falling edge, abscissa scale is 2 V/div and ordinate scale is 2 ns/div.

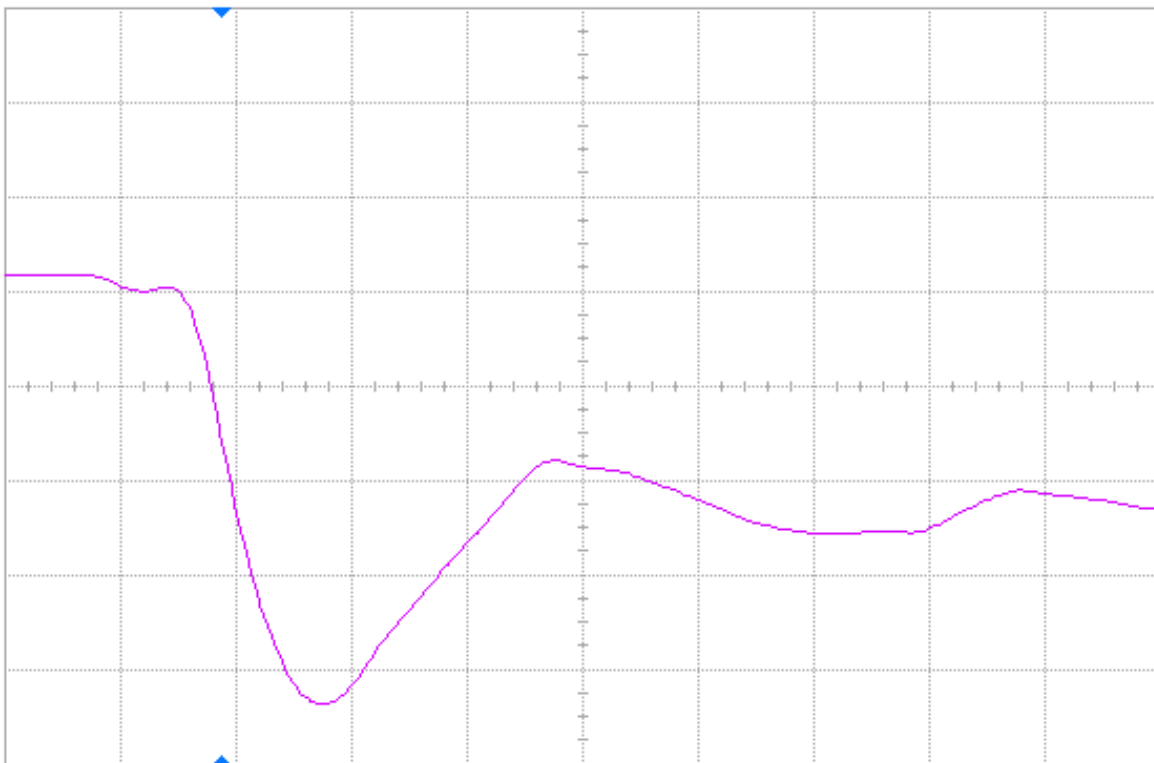


Figure 13(a) DUT 39770 pre-irradiation falling edge, abscissa scale is 2 V/div and ordinate scale is 2 ns/div.

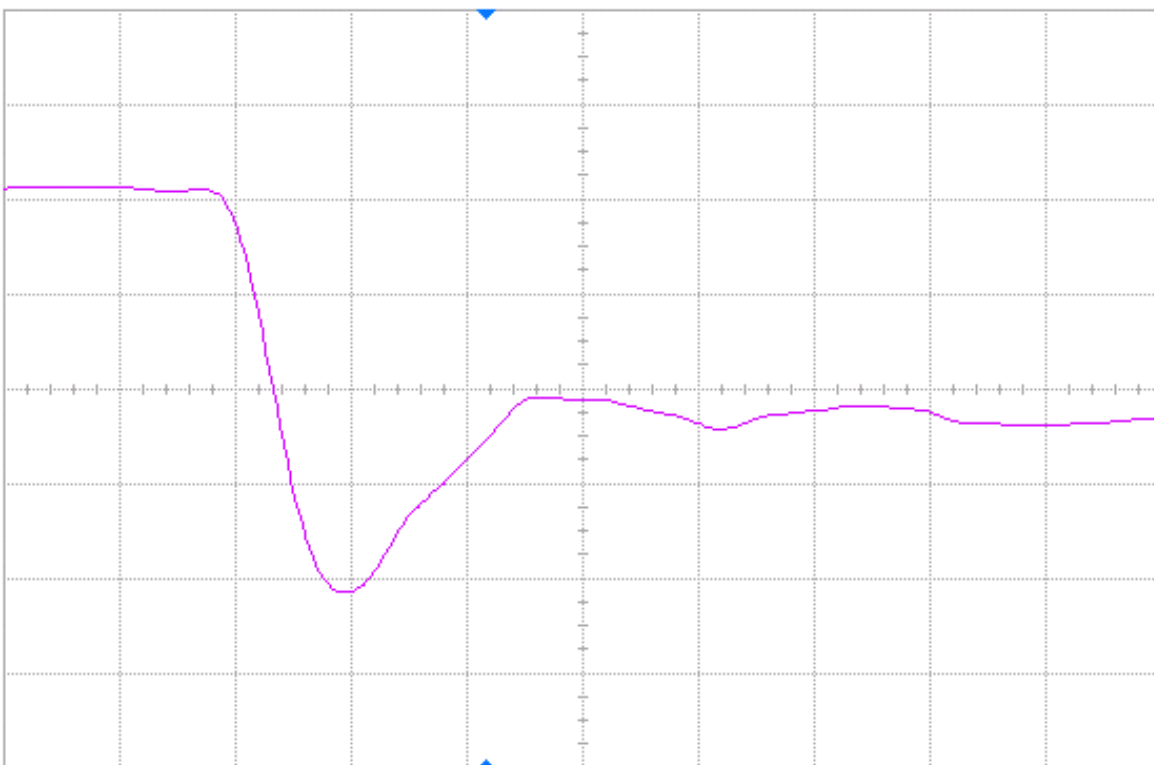


Figure 13(b) DUT 39770 post-annealing falling edge, abscissa scale is 2 V/div and ordinate scale is 2 ns/div.

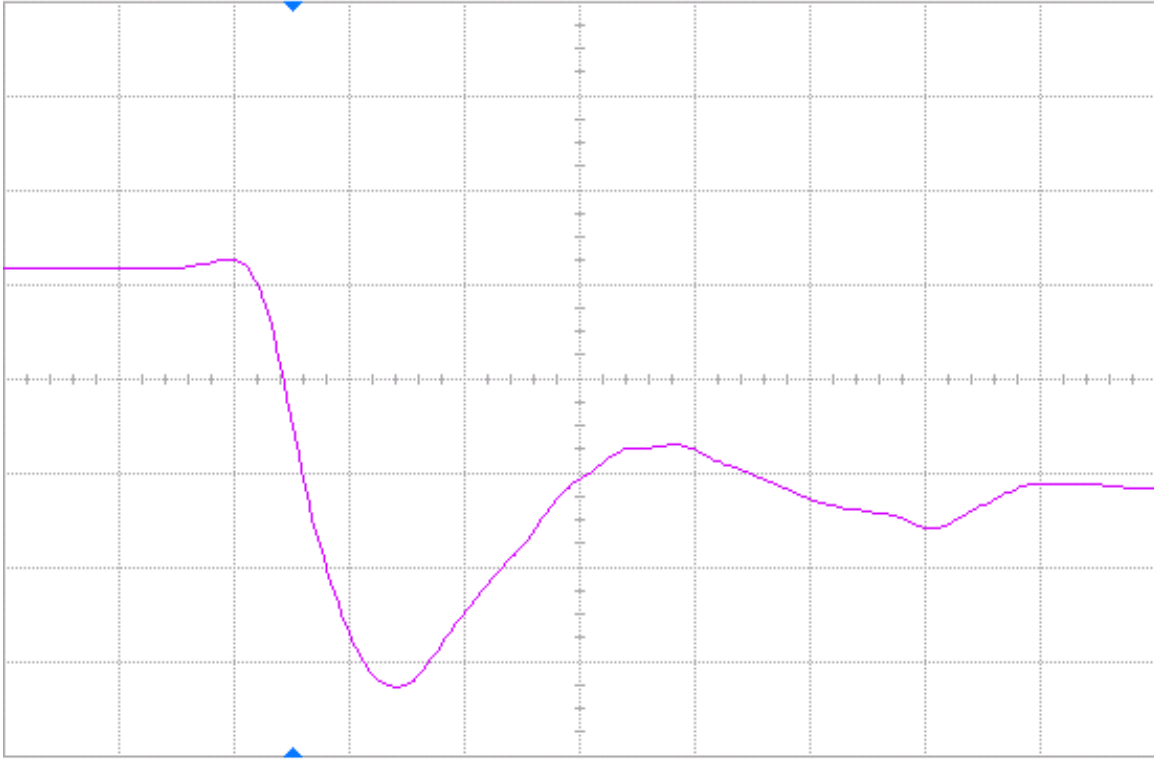


Figure 14(a) DUT 39792 pre-irradiation falling edge, abscissa scale is 2 V/div and ordinate scale is 2 ns/div.

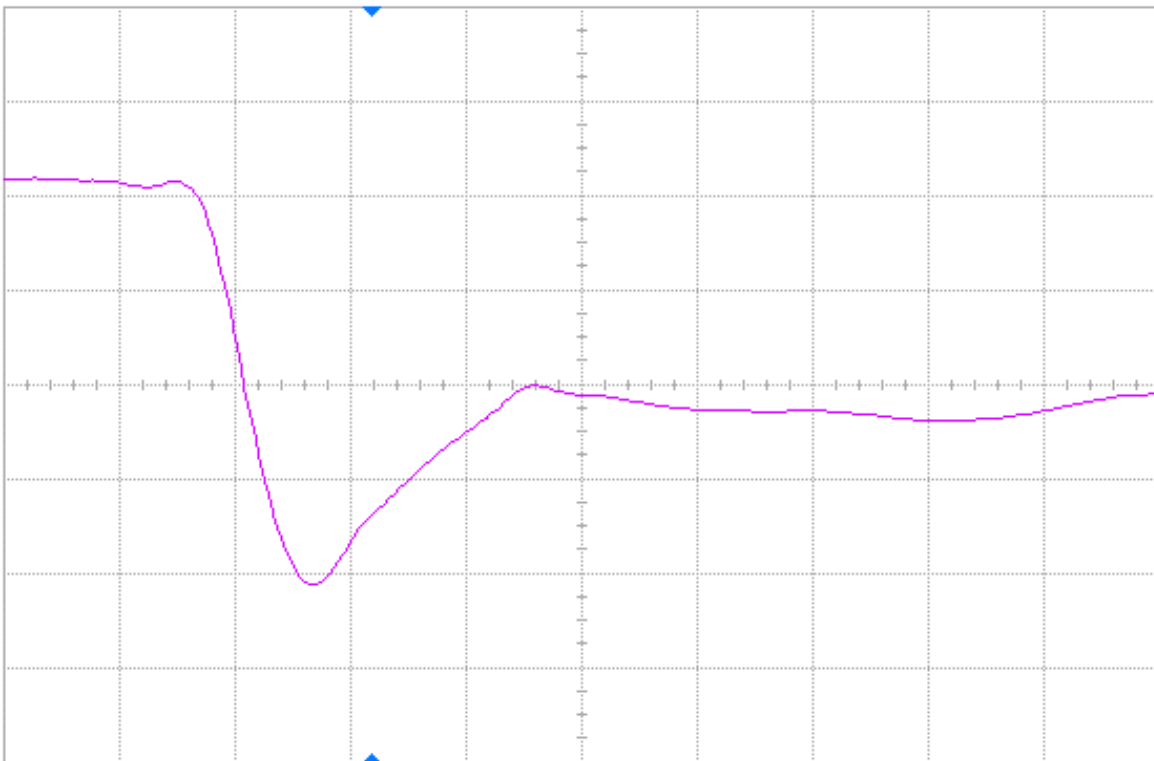


Figure 14(b) DUT 39792 post-annealing falling edge, abscissa scale is 2 V/div and ordinate scale is 2 ns/div.

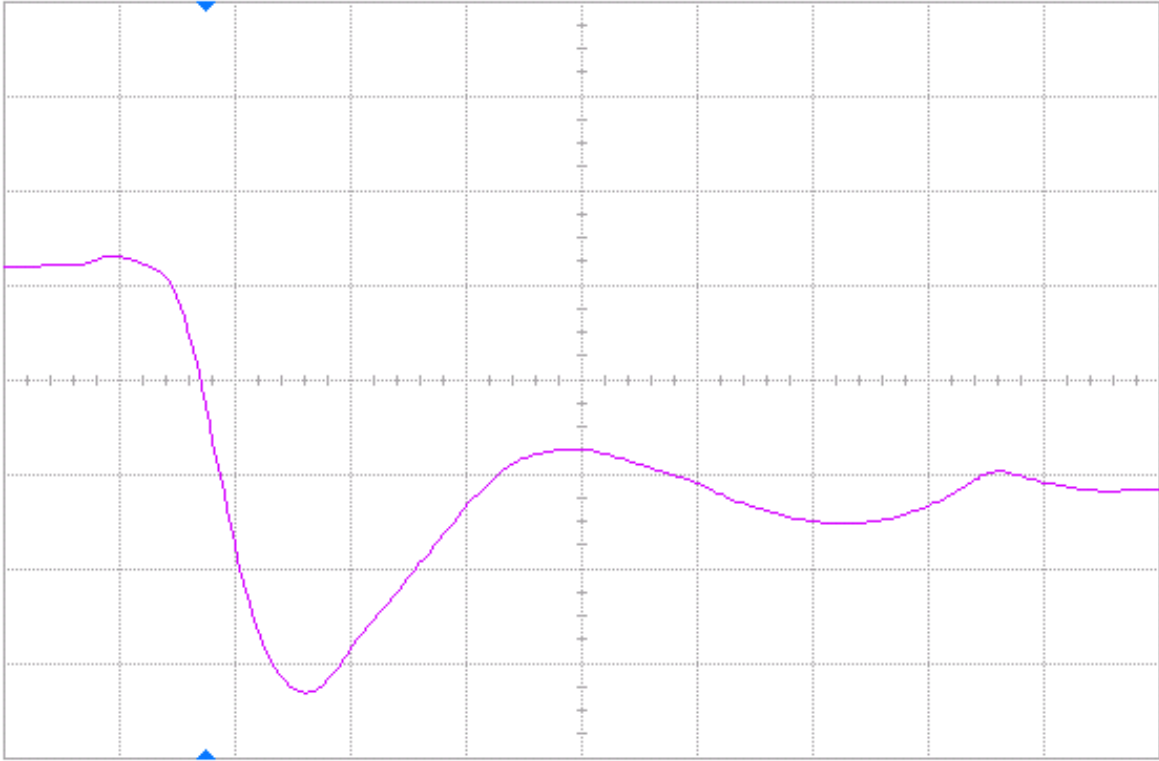


Figure 15(a) DUT 39843 pre-irradiation falling edge, abscissa scale is 2 V/div and ordinate scale is 2 ns/div.

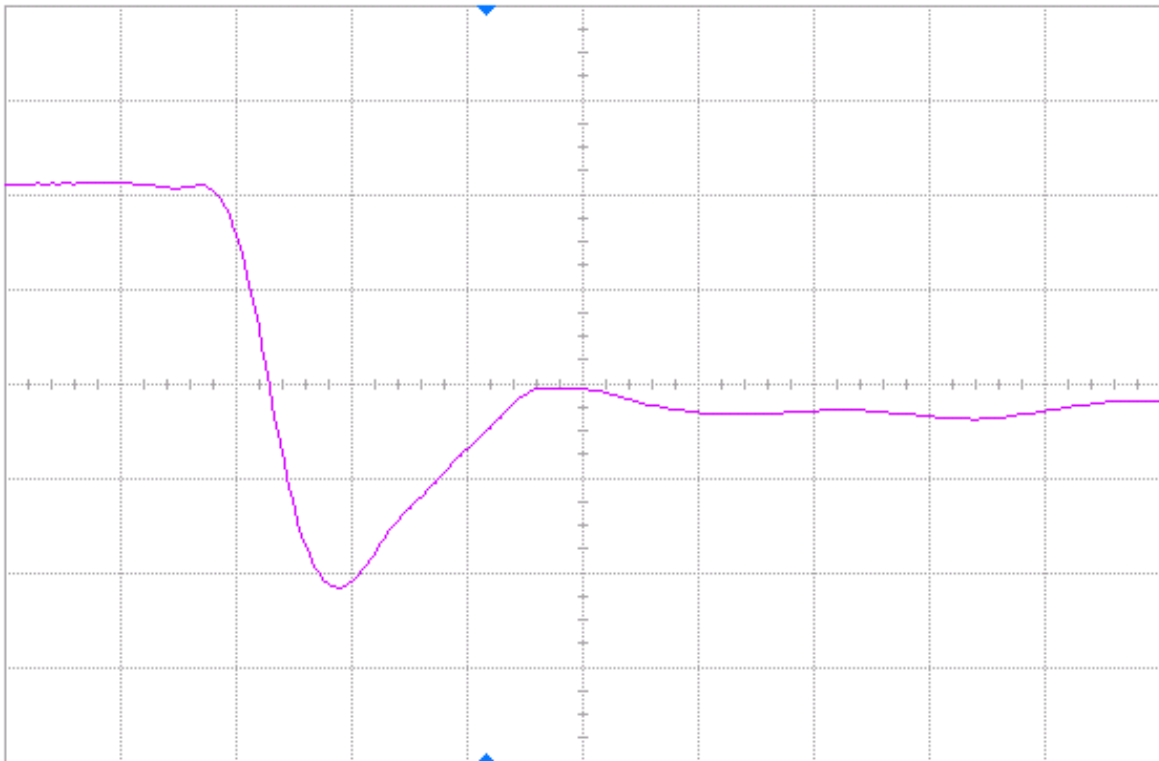


Figure 15(b) DUT 39843 post-annealing falling edge, abscissa scale is 2 V/div and ordinate scale is 2 ns/div.

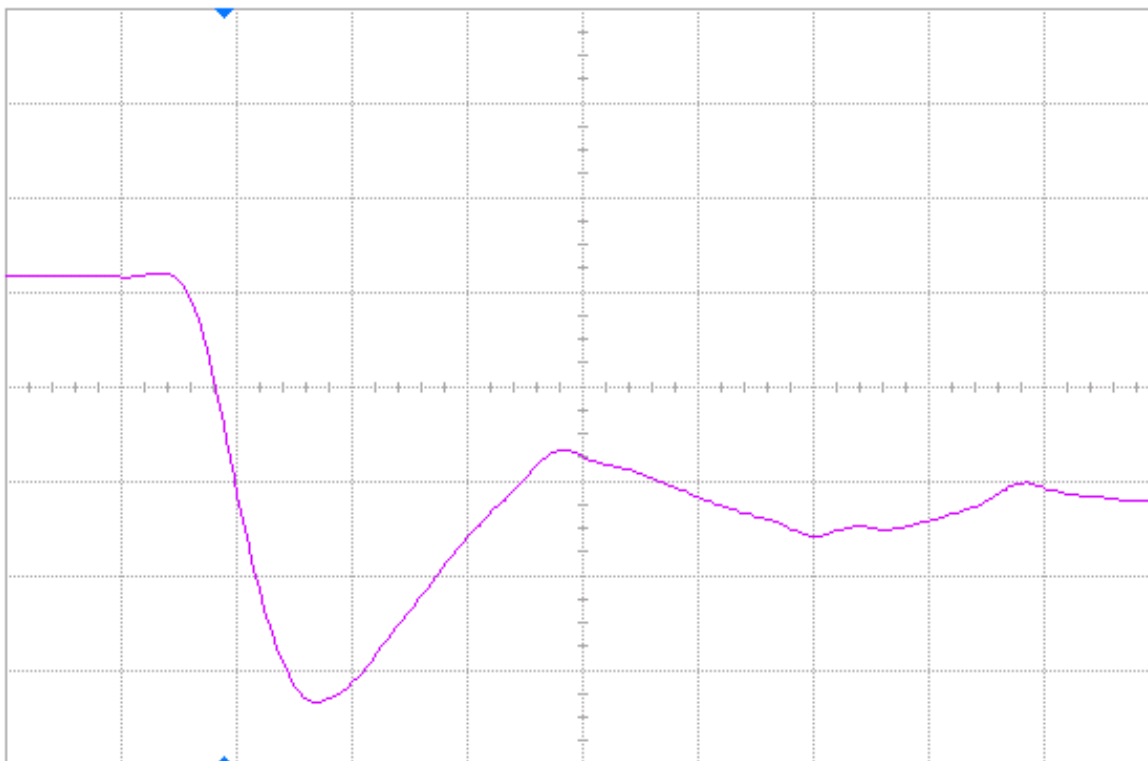


Figure 15(a) DUT 39845 pre-irradiation falling edge, abscissa scale is 2 V/div and ordinate scale is 2 ns/div.

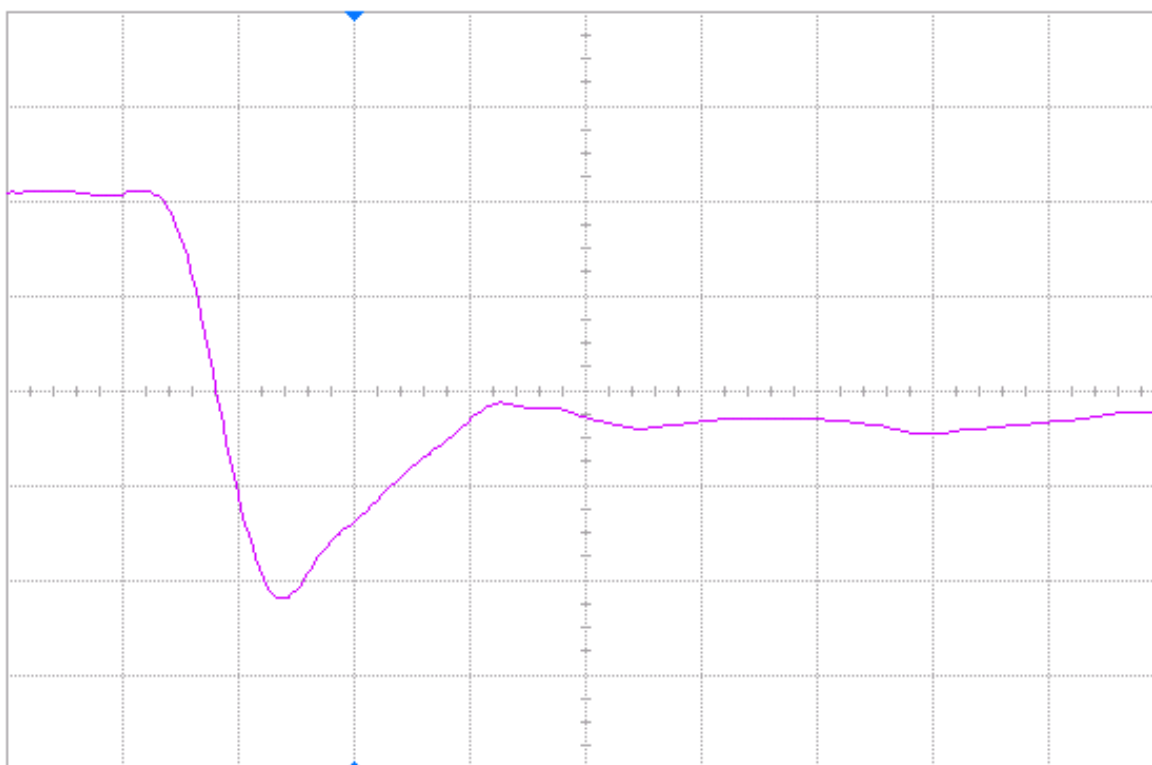
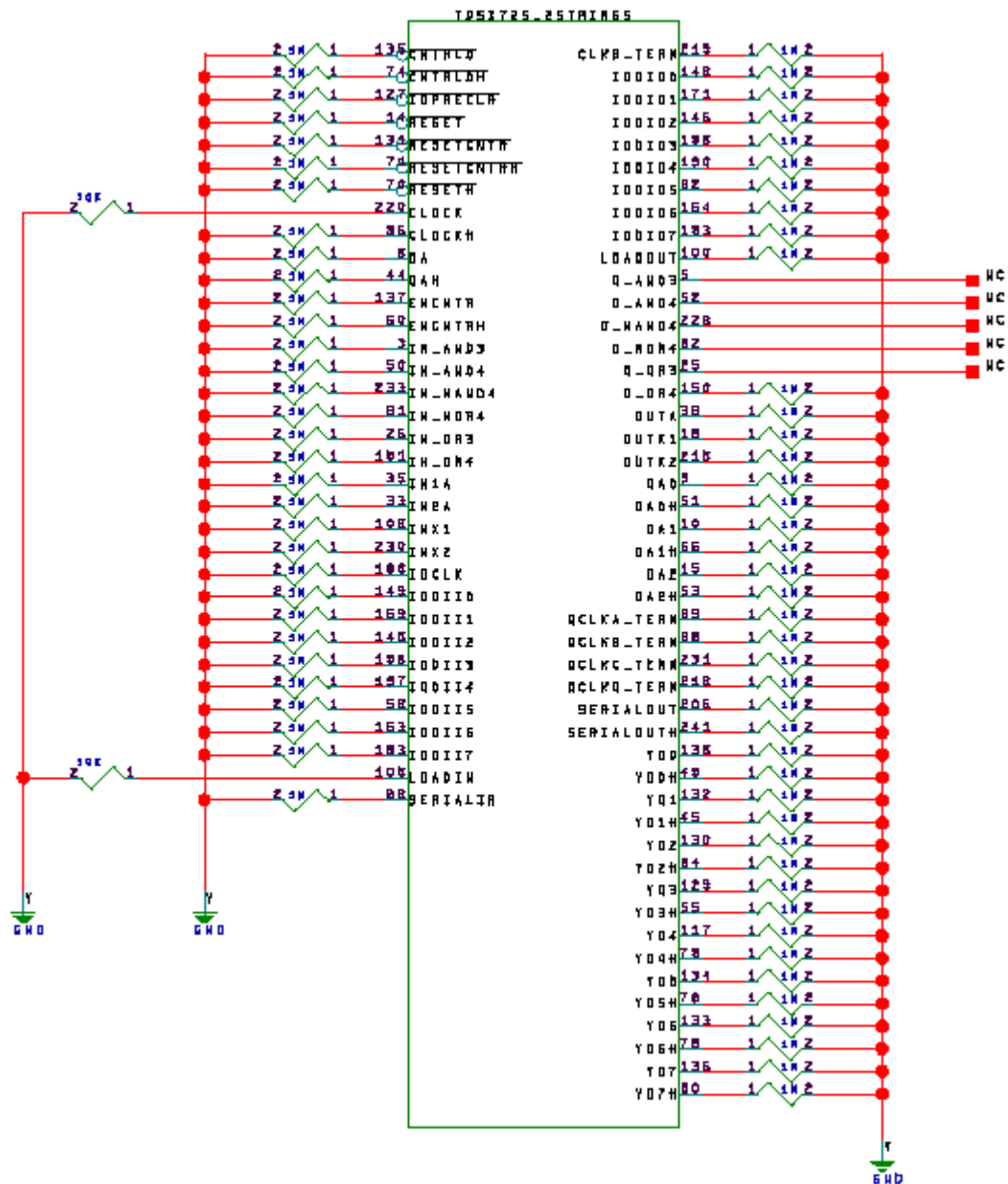
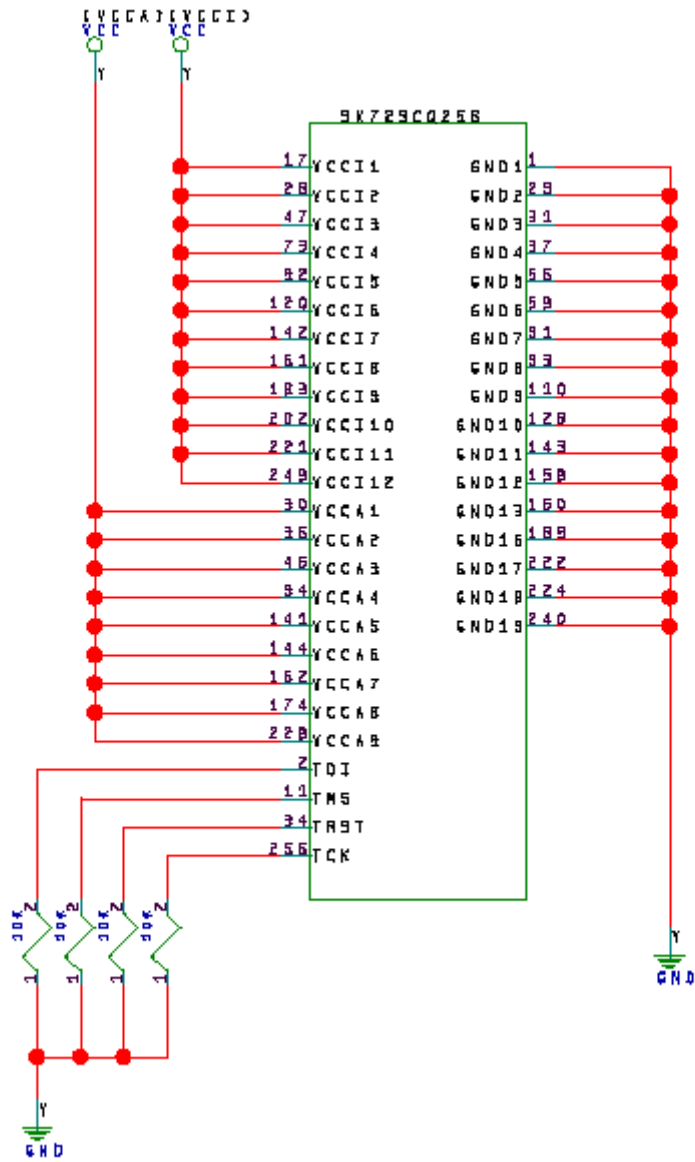


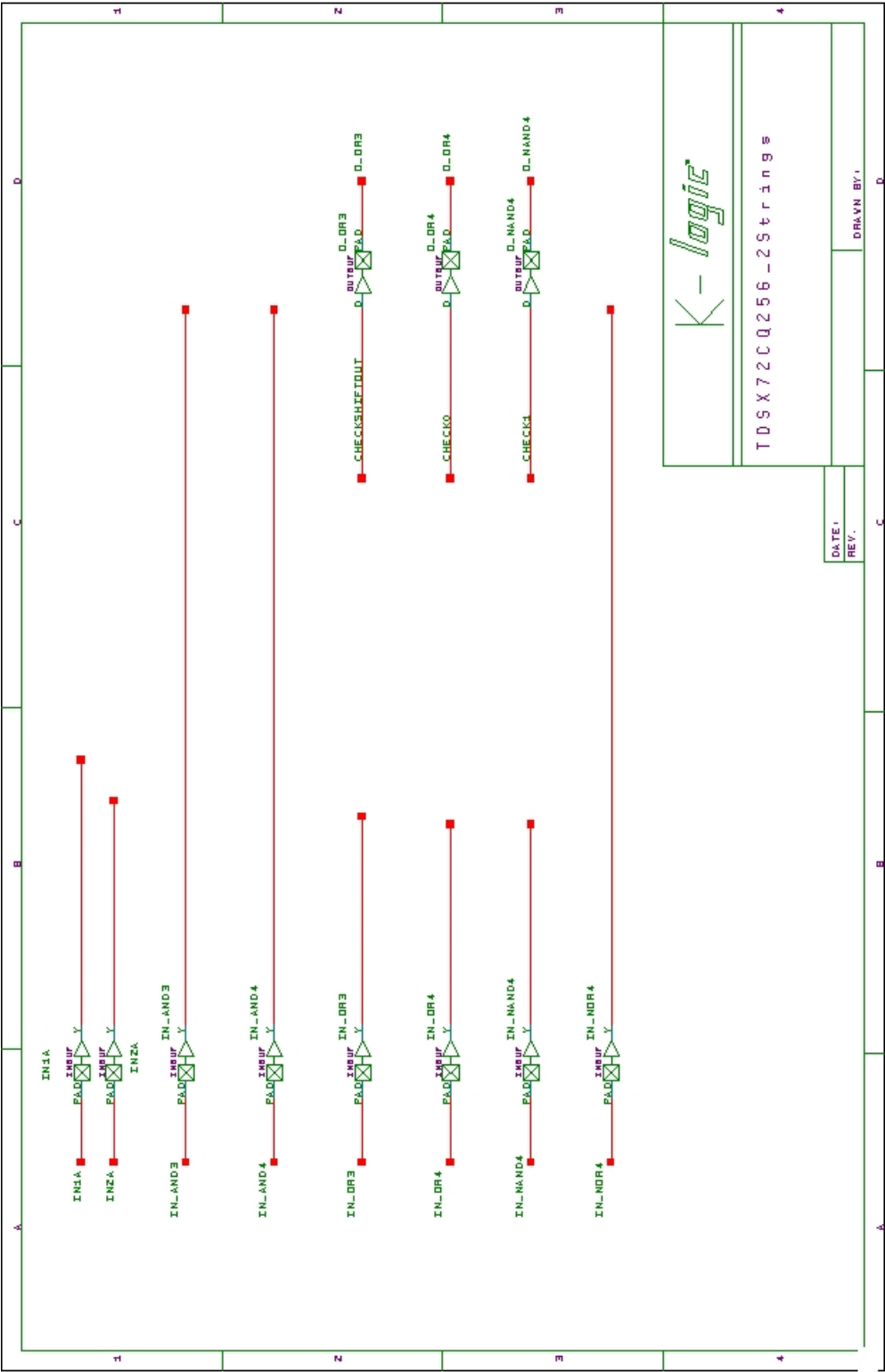
Figure 15(b) DUT 39845 post-irradiation falling edge, abscissa scale is 2 V/div and ordinate scale is 2 ns/div.

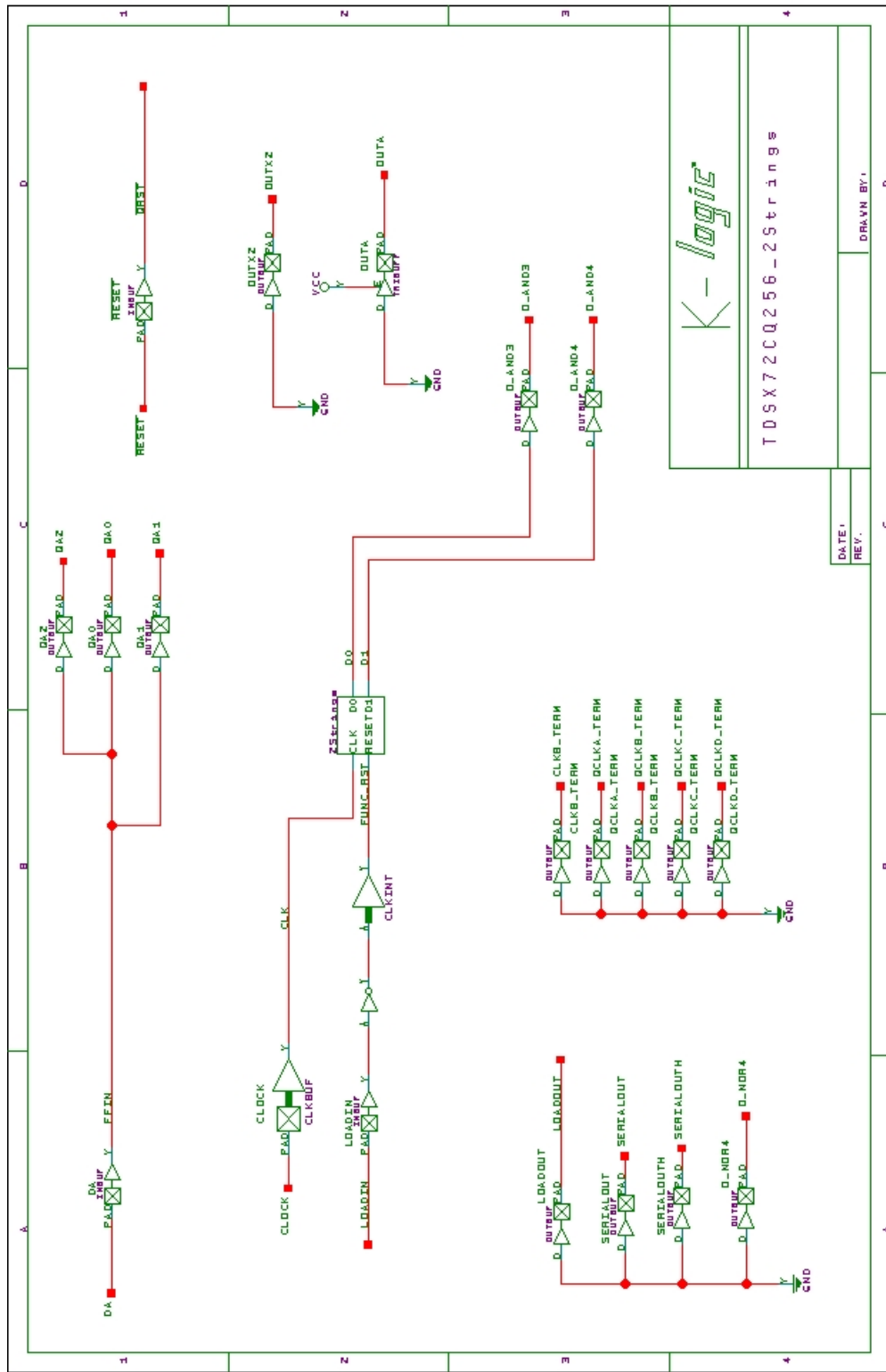
APPENDIX A DUT BIAS

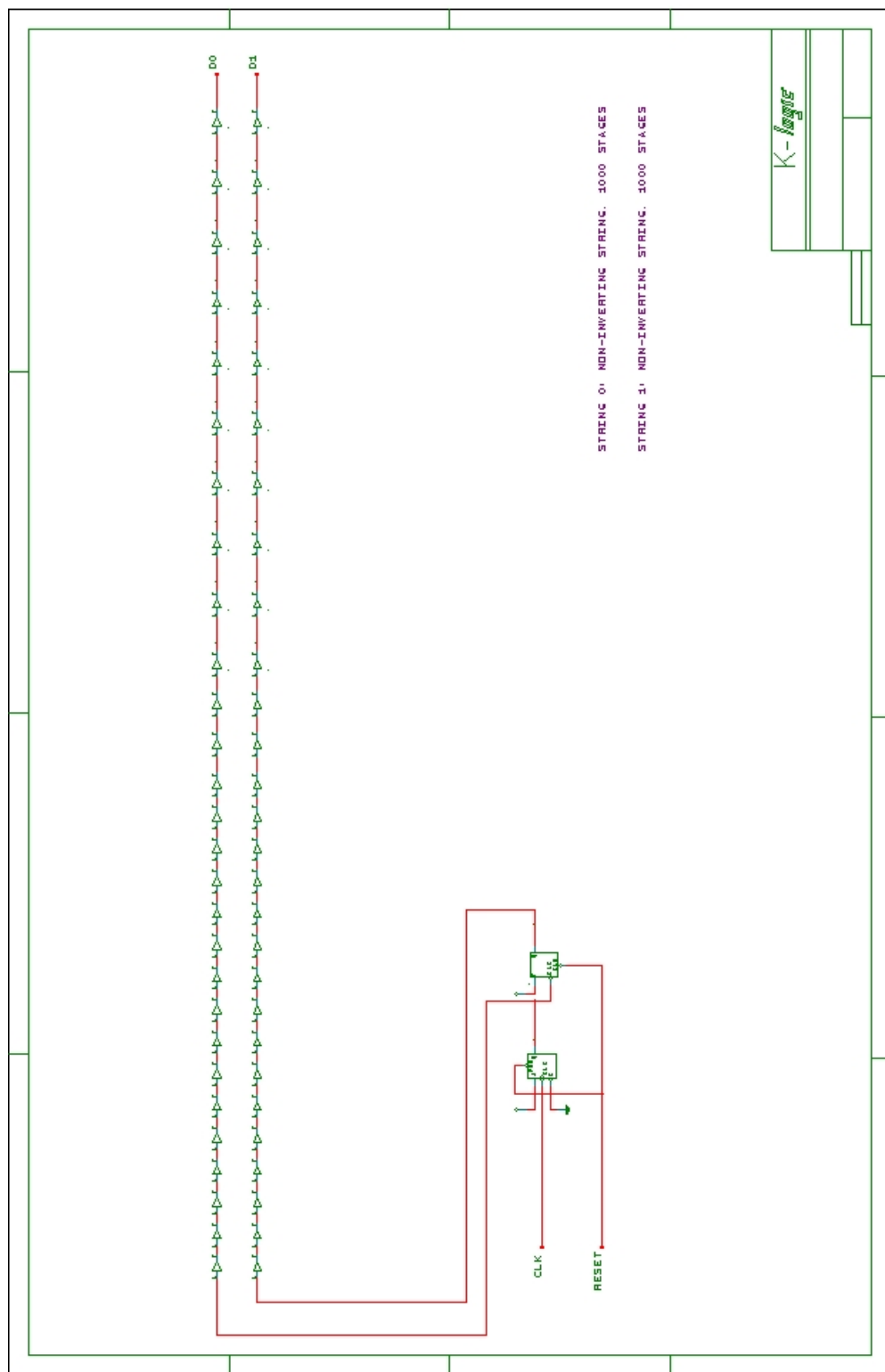




APPENDIX B DUT DESIGN SCHEMATICS







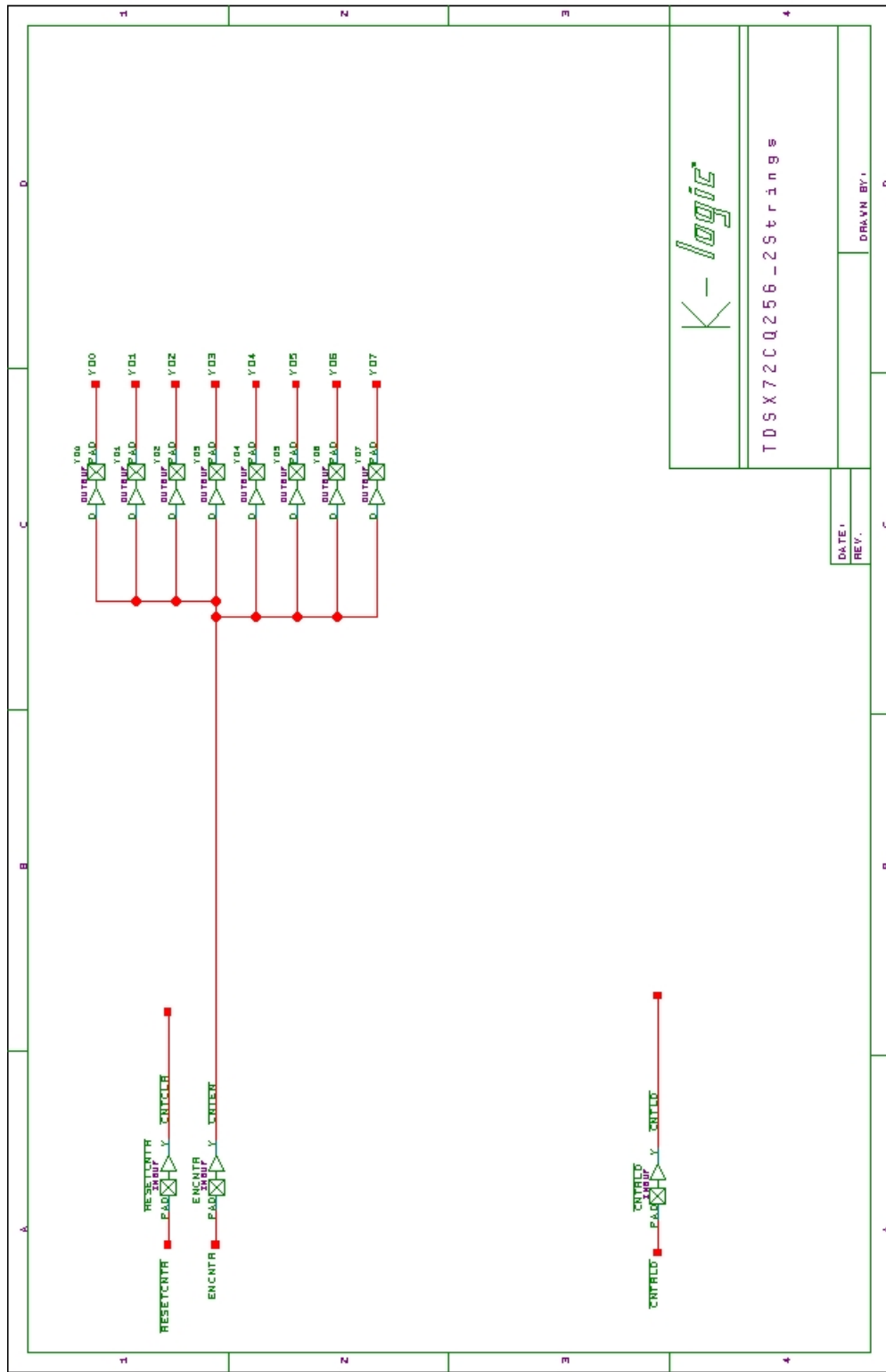


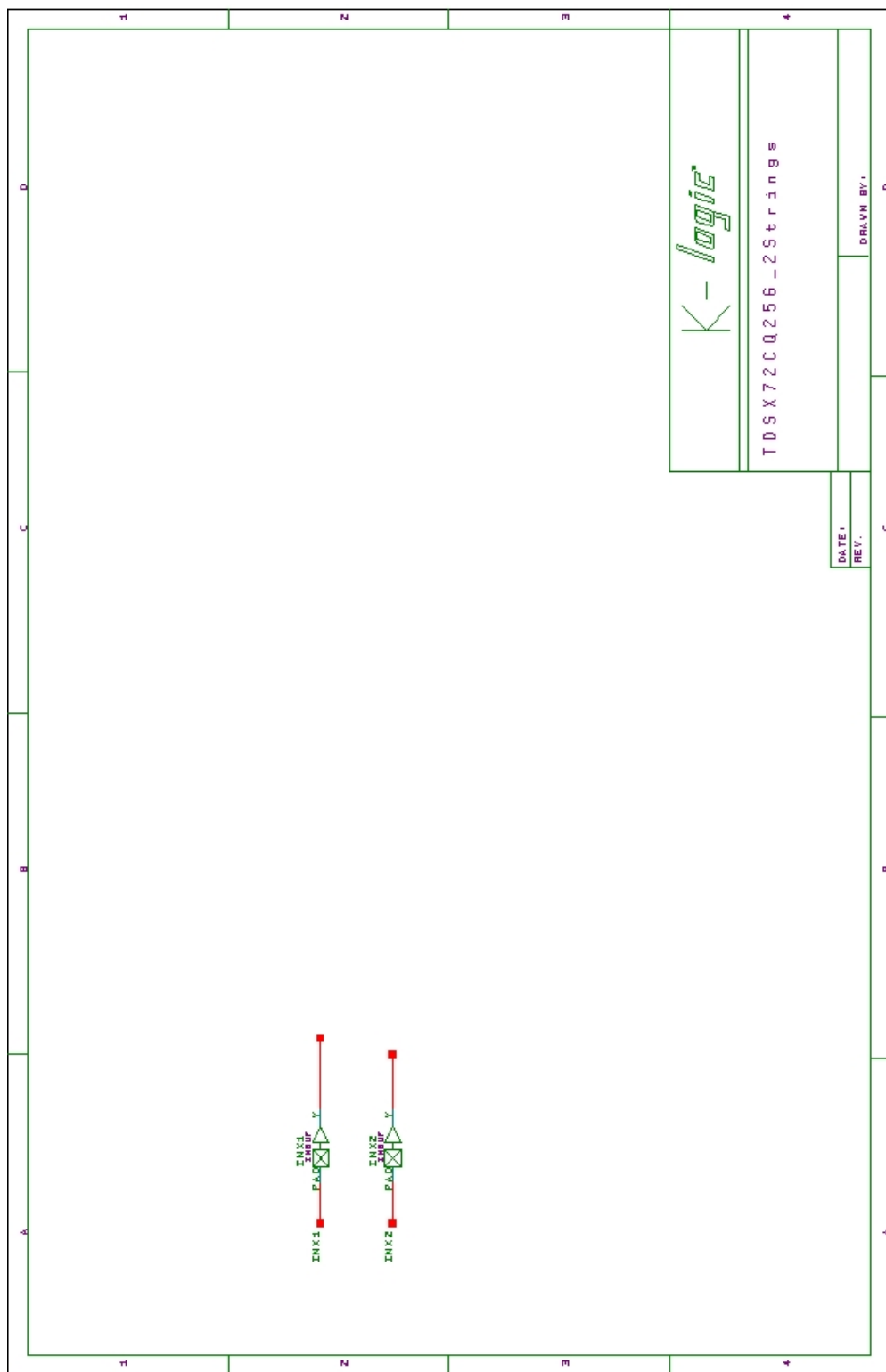
K-logic

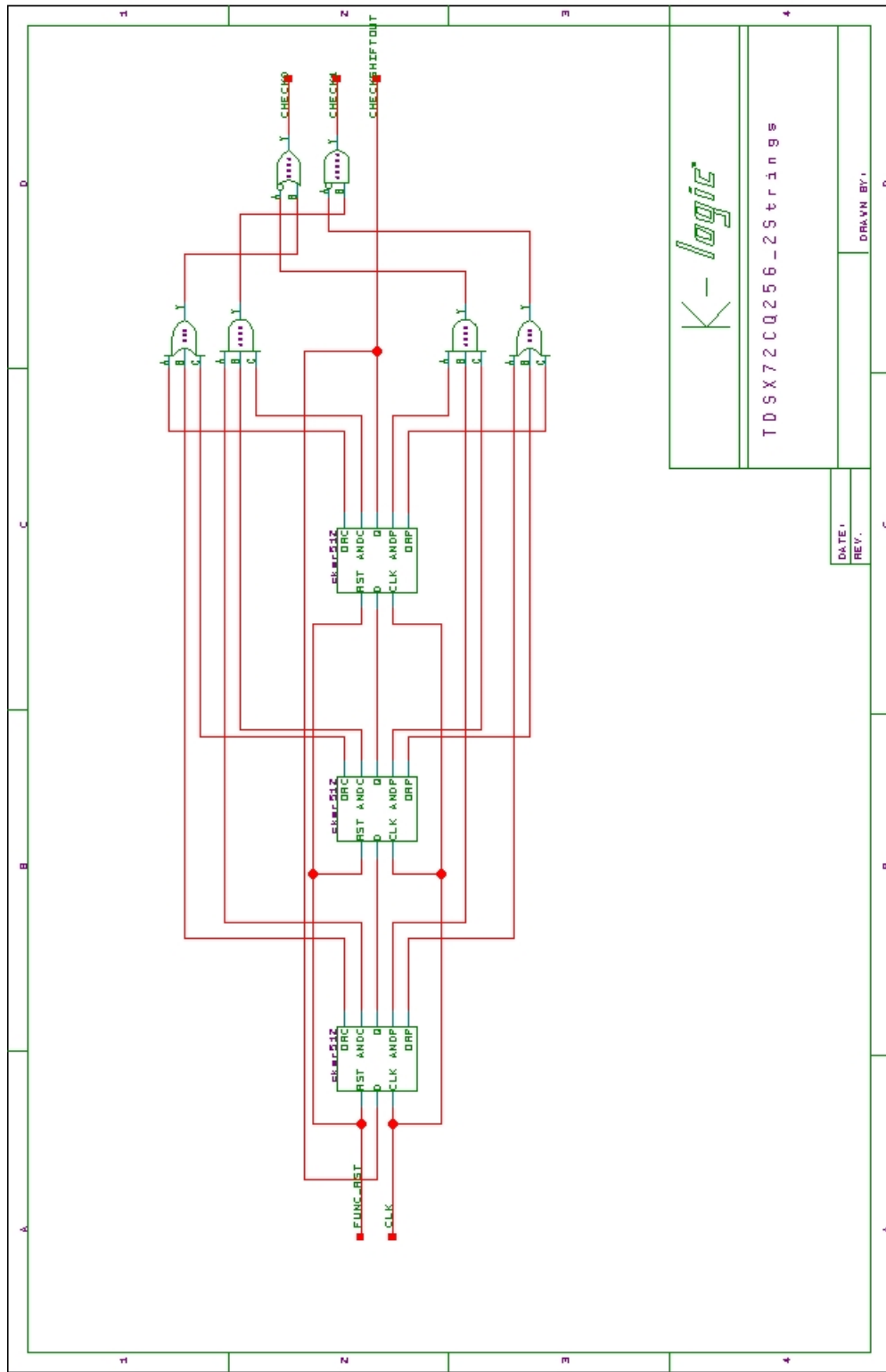
TDACT3SX CQ\BUF50NINV

DATE:
REV.

DRAWN BY: ABK







K-logic	
TDSX72CQ256-2Strings	
DATE:	DRAWN BY:
REV:	

